



**DESIGN AND EVALUATION OF COOPERATIVE ADAPTIVE CRUISE
CONTROL (CACC) FOR THE IMPROVEMENT OF HIGHWAY TRAFFIC
FLOW**

AHMED M. H. AL-JHAYYISH

JANUARY 2016

**DESIGN AND EVALUATION OF COOPERATIVE ADAPTIVE CRUISE
CONTROL (CACC) FOR THE IMPROVEMENT OF HIGHWAY TRAFFIC
FLOW**

**A THESIS SUBMITTED TO
THE GRADUATE SCHOOL OF NATURAL AND APPLIED
SCIENCES OF
ÇANKAYA UNIVERSITY**

**BY
AHMED M. H. AL-JHAYYISH**

**IN PARTIAL FULFILLMENT OF THE REQUIREMENTS FOR THE
DEGREE OF
MASTER OF SCIENCE
IN
THE DEPARTMENT OF
ELECTRONIC AND COMMUNICATION ENGINEERING**

JANUARY 2016

Title of the Thesis : **Design and Evaluation of Cooperative adaptive Cruise Control (CACC) for the Improvement of Highway Traffic Flow.**

Submitted by **AHMED M. H. AL-JHAYYISH**

Approval of the Graduate School of Natural and Applied Sciences, Çankaya University.



Prof. Dr. Halil T. EYYÜBOĞLU
Director

I certify that this thesis satisfies all the requirements as a thesis for the degree of Master of Science.



Prof. Dr. Yusuf Ziya UMUL
Head of Department

This is to certify that we have read this thesis and that in our opinion it is fully adequate, in scope and quality, as a thesis for the degree of Master of Science.



Assoc. Prof. Dr. Klaus Werner SCHMIDT
Supervisor

Examination Date: 21.01.2016

Examining Committee Members

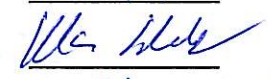
Assoc. Prof. Dr. Orhan GAZİ

(Çankaya Univ.)



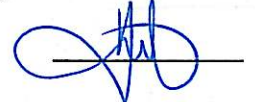
Assoc. Prof. Dr. Klaus Werner SCHMIDT

(Çankaya Univ.)



Assoc. Prof. Dr. Umut ÖRGÜNER

(METU)



STATEMENT OF NON-PLAGIARISM PAGE

I hereby declare that all information in this document has been obtained and presented in accordance with academic rules and ethical conduct. I also declare that, as required by these rules and conduct, I have fully cited and referenced all material and results that are not original to this work.

Name, Last Name : Ahmed, AL-JHAYYISH

Signature : 

Date : 21.01.2016

ABSTRACT

DESIGN AND EVALUATION OF COOPERATIVE ADAPTIVE CRUISE CONTROL (CACC) FOR THE IMPROVEMENT OF HIGHWAY TRAFFIC FLOW

AL-JHAYYISH, Ahmed M. H.

M.Sc., Department of Electronic and Communication Engineering

Supervisor: Assoc. Prof. Dr. Klaus Werner SCHMIDT

January 2016, 59 pages

The subject of intelligent transportation systems (ITS) began to take worldwide attention in the last decade. One main purpose of deploying ITS is the improvement of traffic flow capacity on highways while ensuring safety. Cooperative Adaptive Cruise Control (CACC) is a method used to support the flow of road vehicles at a safe distance in the form of vehicle strings. In order to enable small inter-vehicle spacing, CACC is implemented on each vehicle by the use of vehicle distance measurements as well as information from other vehicles via vehicle-to-vehicle communication. An important goal of CACC is the achievement of string stability in order to attenuate fluctuations in the vehicle motion along vehicle strings. Hereby, CACC designs in the literature are limited to the case of homogeneous vehicle strings, where all vehicles have identical dynamic properties.

In the first part of this thesis, an original CACC H_∞ controller design method is developed for the practical case of heterogeneous vehicle strings while achieving

string stability. The second part of this thesis considers the issue of delay in the CACC control design for platoons of vehicles. Several H_∞ control design methods for time-delay systems are applied to address both communication and vehicle plant delay. For each method, a longitudinal controller for a platoon of vehicles is obtained which results in the achievement of string stability. In addition, a comparison of the different methods regarding the supported delay and inter-vehicle spacings is performed. The findings of the thesis are supported by representative simulation experiments. We note that, to the best of our knowledge, no research has considered the CACC design for heterogeneous vehicles and CACC design with delay.

Keywords: Intelligent Transportation Systems, Cooperative Adaptive Cruise Control, String Stability, Heterogeneous vehicles, CACC with Delay, H_∞ Control.

ÖZ

TRAFİK AKIŞINI İYİLEŞTİRMEK İÇİN KOOPERATİF OTOMATİK SEYİR KONTROLÜNDE DİZAYN VE DEĞERLENDİRME

AL-JHAYYISH, Ahmed M. H.

Yüksek Lisans, Elektronik ve Haberleşme Mühendisliği Anabilim Dalı

Tez Yöneticisi: Doç Dr. Klaus Werner SCHMIDT

Ocak 2016, 59 sayfa

Günümüzde akıllı ulaşım sistemlerine (AUS) olan ilgi giderek artmaktadır. Akıllı ulaşım sistemlerinin geliştirilmesinin ana amacı emniyetli bir şekilde araç yolundaki trafik akışını devam ettirmektir. Kooperatif Adaptif Araç Kontrolü (KAAK), araç dizisinde araçlar arası güvenilir bir mesafede trafik akışının devam etmesini amaçlayan bir metottur. KAAK yöntemiyle araçlar arası en kısa uzaklığı elde edebilmek için her araçtan uzaklık ölçülerini alınır ve araçtan araca haberleşme yöntemiyle araçlar arası uzaklık verileri hesaplanır. KAAK yönteminde dizi boyunca araçta her hangi bir satürasyon ya da dalgalanma olmadan dizi kararlılığının korunması amaçlanmaktadır. Bundan dolayı, KAAK modelleri literatürde aynı dinamik özellikleri gösteren araçlar için kısıtlı bir konudur. Tezin ilk bölümünde, heterojen araçlarda dizi kararlılığını sağlamak için orijinal KAAK H_∞ kontrol dizayn yöntemi geliştirilmiştir. Tezin ikinci bölümünde, KAAK kontrol modeli araç dizisindeki gecikme konusu ile ilgili çalışmaları içermektedir. Zaman-gecikme sistemleri için birkaç H_∞ kontrol dizayn yöntemi hem haberleşme hem de araç gecikme modeli için uygulanmıştır. Her yöntem için, dizi kararlılığı korunarak araç grubunda uzunlamasına kontrolör elde edilmiştir. Aynı zamanda, farklı yöntemler

kullanarak gecikme ve aralar arası uzaklık ile ilgili karşılařtırmalar yapılmıřtır. Tezde bulunan sonuçlar yapılan simülasyonlar ile desteklenmiřtir. řunu belirtmeliyiz ki bildiđimiz kadarıyla, heterojen aralar ve gecikme ile KAAK yöntemi, bu alıřmada ilk defa kullanılmıřtır.

Anahtar Kelimeler: Akıllı Ulařtırma Sistemleri, Kooperatif Otomatik Seyir Kontrolü, Dizi Kararlılıđı, H_∞ Kontrol.



ACKNOWLEDGEMENTS

I would like to express my deep gratitude to my advisor and supervisor, Assoc. Prof. Dr. Klaus Werner SCHMIDT, for his support and guidance throughout this thesis.

I would also like to thank my parents, sisters, brothers and all my friends for their support and love, I would not be able to accomplish this work without them.



TABLE OF CONTENTS

STATEMENT OF NON PLAGIARISM.....	iii
ABSTRACT.....	iv
ÖZ.....	vi
ACKNOWLEDGEMENTS.....	viii
TABLE OF CONTENTS.....	ix
LIST OF FIGURES.....	xii
LIST OF TABLES.....	xv
LIST OF ABBREVIATIONS.....	xvi
 CHAPTERS:	
1. INTRODUCTION.....	1
2. BACKGROUND.....	4
2.1. Intelligent Transportation Systems.....	4
2.2. CACC and Vehicle Following.....	4
2.3. String Stability.....	5
2.4. CACC Control Structure.....	8
2.5. Simulation Example for Homogeneous Vehicles.....	10
2.6. H_∞ control Computation.....	12
3. CACC DESIGN FOR HETEROGENEOUS VEHICLES.....	16
3.1. Longitudinal Vehicle Dynamics.....	16
3.2. Modified Block Diagram.....	18
3.3. String Stability Bounds.....	19
3.4. Controller Design Methods for Heterogeneous Vehicles.....	21
3.5. Simulation Study for Heterogeneous.....	23
3.5.1. CACC Controller Computation.....	23

3.5.2.	Simulation with Heterogeneous Vehicles.....	24
4.	CACC DESIGN WITH TIME-DELAY.....	27
4.1.	Introduction.....	27
4.2.	CACC Model with Delay.....	28
4.3.	Controller Realizations.....	28
4.3.1.	Rational Controller.....	28
4.3.2.	Modified CACC with Predictor.....	30
4.3.3.	Modified String Stability for CACC with Predictor.....	31
4.4.	Padé-Approximation.....	32
4.4.1.	Controller Design by Padé-Approximation.....	32
4.4.2.	Simulation and Experimental Results.....	32
4.5.	Smith-Predictor.....	36
4.5.1.	Modified CACC with Smith-Predictor.....	37
4.5.2.	Modified CACC with Smith Predictor for $\theta=\emptyset$ case.....	38
4.5.3.	Experimental Results.....	39
4.6.	Finite Impulse Response (FIR) Blocks.....	40
4.6.1.	Modified CACC by FIR Block In Same Delays Case.....	41
4.6.2.	String Stability.....	42
4.6.3.	H_∞ Control Structure.....	43
4.6.4.	Simulation Results.....	44
4.7.	A Transformed Standard H_∞ Problem.....	45
4.7.1.	Introduction.....	45
4.7.2.	Transformation.....	46
4.7.3.	H_∞ Control Design with a Single Delay.....	48
4.7.4.	CACC Design by A Transformed Standard H_∞ Problem.....	51
4.7.5.	Simulation Results.....	52
4.8.	Discussion.....	52
4.8.1.	Simulation Results for Comparison	53
4.8.2.	Headway Time Problem.....	54

5. CONCLUSION AND FUTURE WORK.....	59
REFERENCES.....	R1
APPENDICES.....	A1
A. CURRICULUM VITAE.....	B1



LIST OF FIGURES

FIGURES

Figure 1	Vehicle string with CACC	5
Figure 2	Inputs for CACC realization	6
Figure 3	Vehicle string with 7 vehicles	6
Figure 4	Vehicle string with 7 vehicle performing an acceleration/ deceleration maneuver and CACC design that fulfills strict string stability. Each line represents the motion of one vehicle	7
Figure 5	Vehicle string with 7 vehicles performing an acceleration/ decele- ration deceleration maneuver and CACC design that violates strict string stability	8
Figure 6	Feedback loop for CACC	9
Figure 7	H_∞ control design for CACC	10
Figure 8	Vehicle string with 11 vehicles	10
Figure 9	Input signal u_1 of the leader vehicle	11
Figure 10	CACC design for string stability: simulation with homogeneous vehicles	11
Figure 11	System with controller for H_∞ design	12
Figure 12	Structure of cruise control system	17
Figure 13	Feedback loop for CACC	18
Figure 14	Feedback loop for CACC with heterogeneous vehicles.....	22
Figure 15	H_∞ control loop for heterogeneous vehicles	22
Figure 16	CACC simulation with heterogeneous vehicles and strict string stability for first example	25
Figure 17	Zoom in figure for velocity and acceleration of first example	25

Figure 18	CACC simulation with heterogeneous vehicles and strict stability for second example	26
Figure 19	System with delay	27
Figure 20	CACC model with delay	28
Figure 21	H_∞ design for CACC	30
Figure 22	CACC model with predictor	30
Figure 23	String of six vehicles	33
Figure 24	Acceleration input	33
Figure 25	CACC design for 0.1s delay by second-order Padé-approximation.....	34
Figure 26	CACC design for 0.1s delay by fifth-order Padé-approximation.....	34
Figure 27	CACC design for 0.3s delay by second-order Padé-approximation.....	35
Figure 28	CACC design for 0.3s delay by fifth-order Padé-approximation	35
Figure 29	CACC design for 0.5s delay by second-order Padé-approximation.....	35
Figure 30	CACC design for 0.5s delay by fifth-order Padé-approximation	36
Figure 31	System with Smith-predictor loop.....	36
Figure 32	CACC model with Smith-predictor.....	37
Figure 33	Modified CACC in $\Theta=\emptyset$ case	38
Figure 34	Structure of H_∞ control for CACC with Smith-predictor	39
Figure 35	CACC with Smith-predictor design for string stability with 0.1s delay.....	39
Figure 36	CACC with Smith-predictor design for string stability with 0.3s delay.....	40
Figure 37	CACC with Smith-predictor design for string stability with 0.5s delay.....	40
Figure 38	Modified CACC model in same delays case	41
Figure 39	CACC with FIR block.....	42
Figure 40	Modified CACC by using FIR block	43
Figure 41	H_∞ design for CACC with FIR block	44
Figure 42	CACC with FIR block for string stability with 0.1s delay	44
Figure 43	CACC with FIR block for string stability with 0.3s delay.....	45
Figure 44	CACC with FIR block for string stability with 0.3s delay.....	45
Figure 45	General control setup for time-delay systems	46

Figure 46	An equivalent structure	47
Figure 47	The graphic interpretation of the transformation	48
Figure 48	Structure of H_∞ optimal control for CACC model	51
Figure 49	Structure of a transformed standard H_∞ for CACC model.....	52
Figure 50	CACC design by a transformed standard H_∞ with 0.1s delay	53
Figure 51	CACC design by a transformed standars H_∞ with 0.3s delay	53
Figure 52	CACC design by a transformed standars H_∞ with 0.5s delay	54
Figure 53	Design methods for string stability with 0.1s delay	56
Figure 54	Design methods for string stability with 0.3s delay	57
Figure 55	Design methods for string stability with 0.5s delay	55

LIST OF TABLES

TABLES

Table 1	Parameters for the CACC controller design for first example....	23
Table 2	Parameters for the CACC controller design for second example	24
Table 3	Some converted delays by Padé-approximation.....	32
Table 4	Control design for 0.1s delay.....	55
Table 5	Control design for 0.3s delay.....	55
Table 6	Control design for 0.5s delay.....	55
Table A.1	Controllers computation for experiment of chapter 2.....	A1
Table A.2	Controllers computation for first example of chapter 3.....	A1
Table A.3	Controllers computation for experiment of chapter 4.....	A2
Table A.4	Controllers computation for experiment of chapter 4	A3

LIST OF ABBREVIATIONS

ITS	Intelligent Transportation Systems
CACC	Cooperative Adaptive Cruise Control
ACC	Adaptive Cruise Control
V2V	Vehicle to Vehicle
V_i	Velocity of Vehicle i
d_i	Actual Inter-Vehicle Distance of Vehicle i
$d_{r,i}$	Desired Inter-Vehicle Distance of Vehicle i
r_i	Standstill Distance of Vehicle i
h	Time Headway
e_i	Spacing Error of Vehicle i
q_i	Rear Bumper Position of Vehicle i
L_i	Length of Vehicle i
G	Plant of Vehicle
θ	Communication Delay
ϕ	Possible Plant Delay
Γ_i	String-Stability of Vehicle i
τ	Time Constant
H(s)	Spacing Policy
K_{fb}	Feedback Controller
K_{ff}	Feedforward Controller
W	Weighting Transfer Function
S(s)	Closed-Loop Sensitivity
K_{fbo}	Main Feedback Controller
K_{ffo}	Main Feedforward Controller
δ	Mutual Delay between θ and ϕ

\tilde{G}	Dynamic Vehicle when Delay is Active
T	Time-Delay
FIR	Finite Impulse Response Block



CHAPTER 1

INTRODUCTION

Recent advances in automotive engineering aim at fully or partially replacing human driver functionality [1, 2]. Transportation systems are one of the essentially important aspects of our daily life. This is due to the rapidly growing human population and economy [3, 4], and therefore demands of traffic are ever-increasing. Accordingly, there is a need for increasing safety, enhancing mobility and convenience, improving operational performance, reducing congestion, fuel consumption and emissions to arise [2, 5, 6, 7, 8, 9, 10, 11].

Intelligent Transport Systems (ITS) have developed into a profitable solution for the improvement of the operational performance of traffic systems [4, 12]. This includes planning, construction design, operations, safety and so on [12]. Cooperative Adaptive Cruise Control (CACC) is a recently developed technique for automating the longitudinal vehicle motion [13, 14, 15, 16, 17]. Analogous to Adaptive Cruise Control (ACC) [18, 19, 20, 21], CACC allows to travel at a desired vehicle speed and inter-vehicle spacing, hence maintaining a safe distance to predecessor vehicles based on the distance measurements (RADAR or LIDAR). Commonly, a velocity-dependent spacing policy with a constant headway time (time to reach the position of the predecessor vehicle) is chosen. As an extension to ACC, CACC also uses state information of the predecessor vehicles such as acceleration or velocity that is provided via vehicle-to-vehicle (V2V) communication. Accordingly, CACC enables small inter-vehicle distances which is a pre-requisite for high levels of traffic throughput [2, 22, 21].

CACC's level of effectiveness becomes relevant in dense traffic, where vehicles follow their respective predecessor vehicle at small distances in the form of so-called *vehicle strings*. Here, it is highly necessary that the fluctuations in the motion of any vehicle do not have a negative effect on its followers. In particular, it is desired that such fluctuations are attenuated by the follower vehicles which is captured by the for-

mal condition of *string stability* [23, 24]. Throughout the literature, several control methods are proposed for the successful achievement of string stability by the use of CACC [13], [15] uses H_∞ control and [25] proposes a model-predictive control strategy to accomplish string stability. [17, 26] studies the combination of longitudinal and lateral control for vehicle flowing and [16, 14] focus on the impact of communication delays on string stability. It has to be emphasized that all previous studies assume homogeneous vehicles, where string stability is only obtained in the situation where all vehicles have the same dynamic properties. There is a single exception by the work in [24], which considers the possibility of heterogeneous vehicle strings with a size limit.

The first contribution of thesis is the CACC design for string stability under the assumption of heterogeneous vehicles. The proposed method is based on the H_∞ – design for string stability of homogeneous strings in [15]. To this end, we first develop an analysis algorithm, that determines if a given controller design supports string stability. Further, an H_∞ controller design is developed based on the analysis algorithm. The method used involves a particular weighting transfer function in order to obtain string stability for a wide range of vehicle dynamics and arbitrarily long strings.

Secondly, this thesis contributes to the use of H_∞ control with explicit consideration of delays in the CACC design. There are two such delays in the CACC design: the delay caused by the wireless communication from predecessor vehicles and the internal delay of the plant dynamics [13]. In general, time-delay on CACC affects the stability of the closed-loop and string stability of vehicle platoons [27]. The existing literature only uses a Padé-approximation to include the delays in the CACC design by H_∞ control [15]. This thesis offers various methods for the CACC design including delay by H_∞ control. The first method involves the designing of a H_∞ control by the use of a Smith-predictor. That is, a predictor is added to the closed-loop of the CACC model, eliminating delays from the closed loop. In the second method, the CACC feedback loop is extended by Finite Impulse Response (FIR) blocks. Lastly, a CACC design based on a transformed standard H_∞ problem is applied [28]. This method is based on a transformation of the feedback loop with delay which simplifies the evaluation of the H_∞ norm with delay. With this transformation, the infinite dimensional robust control problem (with delay) can be solved analogous to the finite-dimensional problem. For comparison, we also employ the Padé-approximation, where delays are approxi-

mated by rational transfer function. The properties of the different CACC designs are illustrated by extensive simulation experiments in Matlab/Simulink. Also, a thorough comparison shows the suitability of the different methods regarding different delays and headway times. The controllers for each design are presented in the table at the end of this thesis.

This thesis is organized as follows. Chapter 2 provides background information. In Chapter 3, the CACC design for heterogeneous vehicles is presented. Chapter 4 contains the CACC design with time-delay. Chapter 5 gives conclusion and directions for future work.



CHAPTER 2

BACKGROUND

2.1 Intelligent Transportation Systems

The ever-growing demands of traffic during the last few decades exceeds existing road transportation infrastructure and resources. This leads to increased frequency and severity of traffic problems, such as traffic congestion, traffic accidents and environmental pollution [3]. For these reasons, a robust solution in the future lies in efficient application of presently available means of road transportation and infrastructure [12]. Intelligent transportation systems (ITS) are a possible solution to reduce these issues. ITS can be classified as traffic infrastructure based, vehicle categories based, diverse roads based, vehicle to road based or vehicle to vehicle based technologies [1, 29, 11, 4]. This thesis focuses on the vehicle to vehicle based technologies (vehicles in platoon) of ITS with the design of cooperative adaptive cruise control (CACC) systems to improve the highway traffic flow [30]:

- Increasing the road capacity by small inter-vehicle distances (traffic throughput).
- Increase driving safety.

2.2 CACC and Vehicle Following

Cooperative adaptive cruise control (CACC) takes an important role in the developing traffic flow; the wirelessly communicated data are used in a feedforward setting such that vehicles follow each other in so-called *vehicle strings* at small inter-vehicle spacing [13, 30] as shown in Figure 1.

L_i , q_i and v_i denote the length, rear bumper position and velocity of vehicle i , respectively. Here d_i is the gap between vehicle $i - 1$ and vehicle i . It is assumed that d_i can be measured by vehicle i via using sensors (RADAR or LIDAR) [1, 15, 30]. In addition,

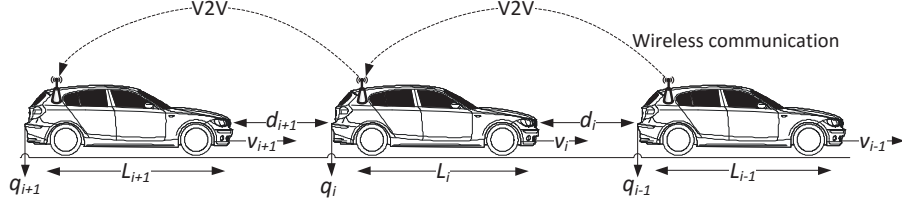


Figure 1: Vehicle string with CACC.

data such as the acceleration or velocity of other vehicles can be obtained via wireless communication with the nearest vehicle (vehicle-to-vehicle (V2V)) communication.

$$d_i(t) = q_{i-1}(t) - q_i(t) - L_i. \quad (2.1)$$

A frequently used spacing policy for CACC is given by the constant headway time policy [15] as shown in (2.2).

$$d_{i,r} = r_i + h v_i. \quad (2.2)$$

Here, $d_{i,r}$ represents the desired spacing between vehicle $i-1$ and vehicle i . It depends on the distance at standstill r_i and the headway time h_i . That is, at zero velocity, the desired distance is r_i and $d_{i,r}$ increases proportional to v_i . The spacing error $e_i(t)$ is then equal to:

$$e_i(t) = d_i(t) - d_{i,r}(t) = (q_{i-1}(t) - q_i(t) - L_i) - (r_i + h v_i(t)). \quad (2.3)$$

2.3 String Stability

The major goal of vehicle-following in dense traffic, (which is essential using CACC), is subject to requirements related to safety, comfort and scalability with respect to platoon length [13]. In order to fulfill these requirements, the vehicle platoon is desired to exhibit string-stable behavior. The CACC must be designed such that disturbances are attenuated along a vehicle string as depicted in Figure 2. That is, a small variation in the speed or acceleration of any vehicle i should not lead to increasing variations in the motion of its follower vehicles. This is equivalent to distance errors that are not

amplified upstream from vehicle to vehicle in a platoon [15, 31].

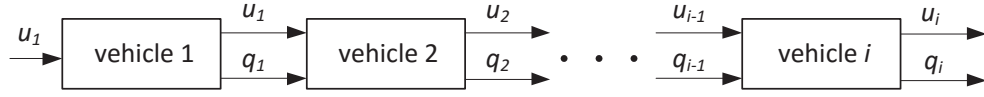


Figure 2: Inputs for CACC realization.

The stated condition is captured by the notion of strict string stability in the literature [15, 16, 17, 23, 24]. Assuming a linear system representation with input u_{i-1} of the preceding vehicle, we write

$$\Gamma_i(s) = \frac{U_i(s)}{U_{i-1}(s)}. \quad (2.4)$$

for the transfer function between the control inputs u_{i-1} and u_i of successive vehicles. Consequently strict string stability is achieved if for all vehicles i

$$\|\Gamma_i(s)\|_\infty \leq 1. \quad (2.5)$$

Hereby, $U_i(s)$ denotes the Laplace transform of the signal $u_i(t)$ and $\|\bullet\|_\infty$ denotes the H_∞ -norm. Hence, each CACC controller design should ensure (2.5). This condition is only addressed for homogeneous vehicles in the literature. This thesis will find a solution for CACC design in the heterogeneous case (different vehicles) and perform a CACC design including communication and plant delays in the next chapters.

In order to clarify the idea of string stability, we present some simulations examples for the case with string stability and the case when string stability is violated. We simulate a string of 7 vehicles as shown in Figure 3. The leader vehicle 1 first accelerates



Figure 3: Vehicle string with 7 vehicles.

with up to 4 m/s² and then decelerates with up to -4 m/s² (right-hand plot). In Figure

4, strict string stable is achieved: the follower vehicles perform the same motion as the leader vehicle with a decreased (attenuated) acceleration/deceleration. In addition the position plot (left-hand side) indicates that the vehicles follow each other at a safe distance. Similarly, the velocity variation (center plot) is attenuated along the vehicle string. This argument is clearly explained by figures. Each vehicle (there is a line for each vehicle) is following its predecessor without amplification in the acceleration or velocity in the platoon. In contrast, string stability is violated in the scenario of Figure

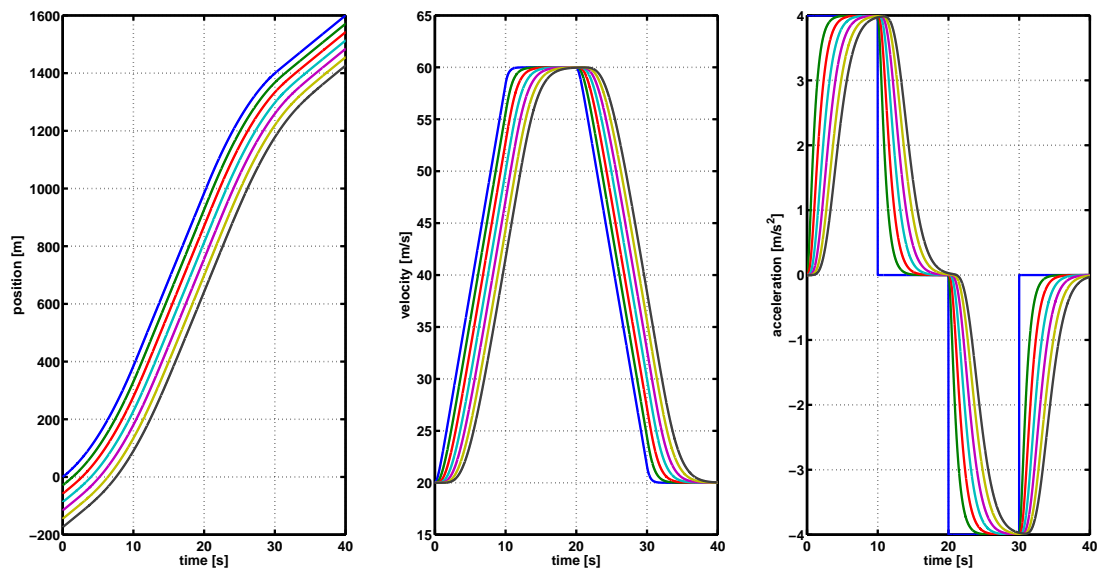


Figure 4: Vehicle string with 7 vehicles performing an acceleration/deceleration maneuver and CACC design that fulfills strict string stability. Each line represents the motion of one vehicle.

5. Performing the same maneuver of the leader vehicle 1, it now holds that the acceleration and velocity of the follower vehicles are amplified which is clearly undesirable. It is evident that the signals of vehicle 2 (which is represented by the green line) are amplified compared to its predecessor vehicle 1 (which is represented by the blue line) and each vehicle follows its predecessor vehicle with amplification. In addition the position plot (left-hand side) shows that the vehicles follow each other at an extremely unsafe distance.

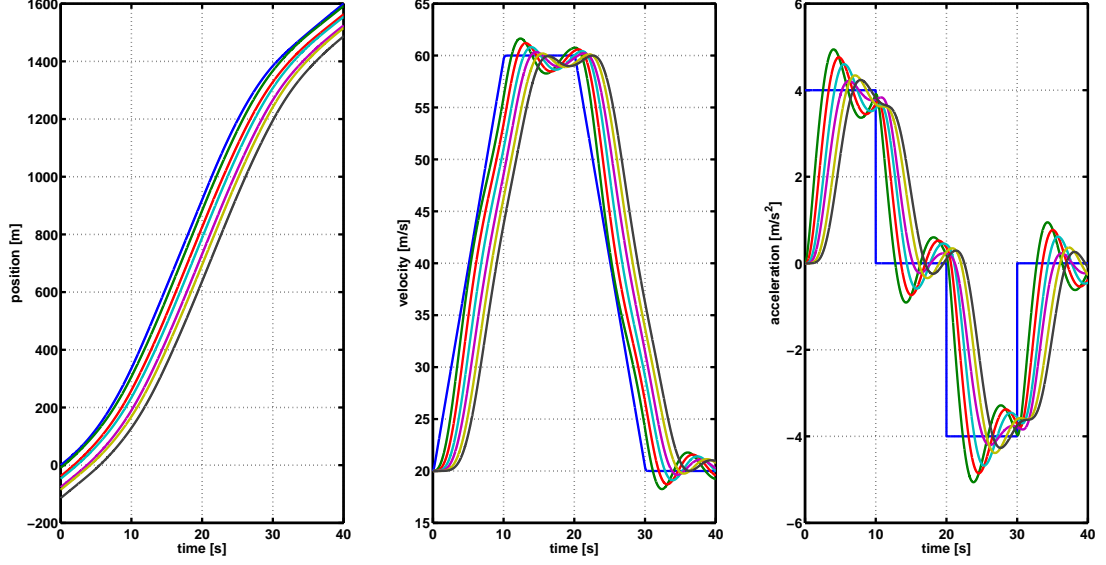


Figure 5: Vehicle string with 7 vehicles performing an acceleration/deceleration maneuver and CACC design that violates strict string stability.

2.4 CACC Control Structure

The CACC design is an extension of standard Adaptive Cruise Control (ACC), feeding additional data by wireless communication to allow short-distance automatic vehicle following. The control objective in this chapter is, as in the literature, only for the case of homogeneous strings, where all vehicles have the same dynamic properties [15, 16]. The most recent approaches [15] use the spacing policy in (2.2) and model each vehicle by the plant transfer function in (2.6).

$$G_i(s) = \frac{e^{-\theta_i s}}{(1 + s \tau_i) s^2} = \frac{Q_i(s)}{U_i(s)}. \quad (2.6)$$

θ_i is a possible plant delay and τ_i is the time constant of the low-level driveline dynamics. Then, a CACC controller is designed for the feedback loop in Figure 6. Here, the input signal u_{i-1} of vehicle i is transmitted to vehicle i via V2V communication and $D = e^{-\phi s}$ represents a potential communication delay. $H = 1 + h s$ is used to implement the spacing policy in (2.2) with the constant headway h and K is the controller transfer matrix which can be written as

$$K = \begin{bmatrix} K_{ff} & K_{fb} \end{bmatrix}. \quad (2.7)$$

K_{ff} is a feedforward controller transfer function for controlling acceleration data by wireless communication and K_{fb} is a feedback controller transfer function for controlling the spacing error $e_i(s)$ between the desired distance and the actual distance. For

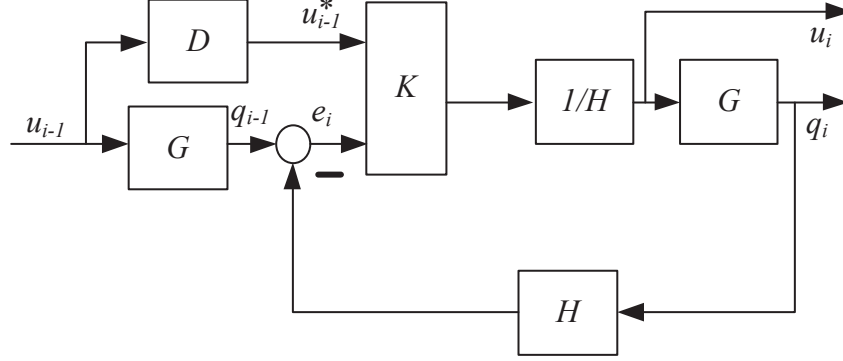


Figure 6: Feedback loop for CACC.

the case of homogeneous vehicles, it holds that $\tau_i = \tau_{i-1}$ and $\theta_i = \theta_{i-1}$ for any vehicles $i, i-1$. Then, the same transfer function Γ is found from Figure 6 for all i :

$$\Gamma(s) := \Gamma_i(s) = \frac{U_i(s)}{U_{i-1}(s)} = \frac{DK_{ff} + G_i K_{fb}}{H(1 + G_i K_{fb})}. \quad (2.8)$$

Hence, according to (2.4), the design of K requires that

$$\|\Gamma(s)\|_\infty \leq 1. \quad (2.9)$$

In addition, [15] considers the closed-loop sensitivity as

$$S(s) = \frac{E_i(s)}{U_{i-1}(s)} = \frac{G(1 - DK_{ff})}{1 + GK_{fb}}. \quad (2.10)$$

In order to fulfill string-stability, (2.9) has to be fulfilled. At the same time, it is desired to minimize the position error $e_i(t)$. Hence, the H_∞ control problem

$$\min_K \left\| \begin{array}{c} \Gamma(s) \\ S(s) \end{array} \right\|_\infty \leq 1 \quad (2.11)$$

is solved. The lower fractional transformation (LFT) and the corresponding matrix P are shown in Figure 7.

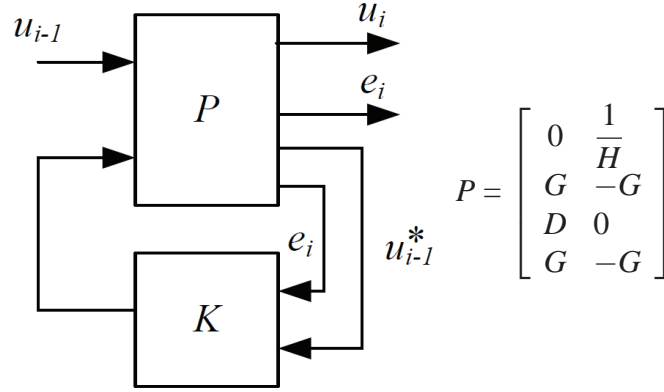


Figure 7: H_∞ control design for CACC.

2.5 Simulation Example For Homogeneous Vehicles

Our simulation platform is based on MATLAB/SIMULINK to evaluate the performance of CACC for homogenous vehicle strings. An example experiment is accomplished for 11 vehicles as shown in Figure 8. In order to quantify values of τ_i , we



Figure 8: Vehicle string with 11 vehicles.

refer to practical experiments in [13], where a value of $\tau \approx 0.4$ is obtained. That is, we choose $\tau_i = 0.4$ for each vehicle and design K according to (2.11). In our simulation, the leader vehicle is provided with the input signal in Figure 9. That is, sharp accelerations of 4 m/s^2 and -4 m/s^2 are given in order to study a difficult vehicle following scenario. The simulation result is shown in Figure 10. It can be seen from the vehicle positions that each vehicle follows its predecessor at a safe distance. In addition, the velocity and acceleration plot suggest that the disturbance provided by the input signal is attenuated along the string (the respective signal amplitudes decrease along the string). That is, strict string stability is confirmed.

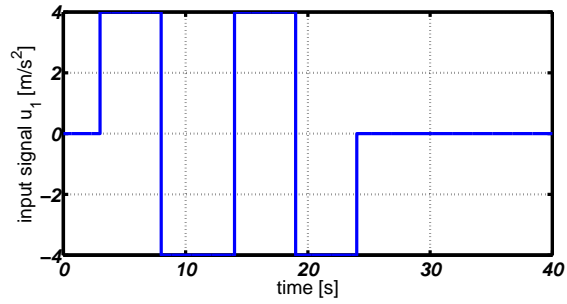


Figure 9: Input signal u_1 of the leader vehicle.

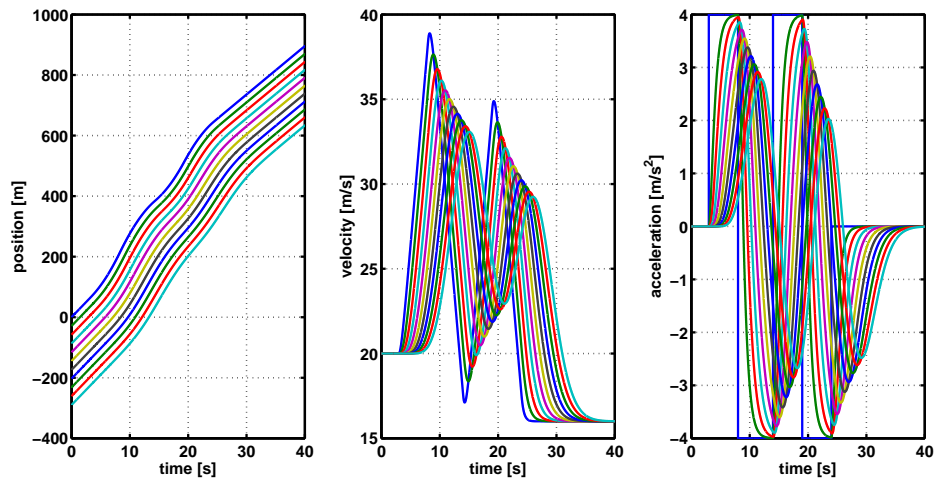


Figure 10: CACC design for string stability: simulation with homogeneous vehicles.

2.6 H_∞ Control Computation

The results in this thesis are based on the H_∞ control design. The optimal H_∞ control is to find all admissible controllers $K(s)$ such that the H_∞ norm of the complementary sensitivity transfer function $\|T_{(zw)}\|$ (between input signal w and output signal z) is minimized as shown in Figure 11. We summarize the necessary computations for the general case as shown in [32].

Assume the interconnected plant P and a general controller $K(s)$.

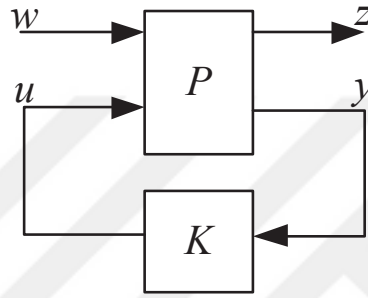


Figure 11: System with controller for H_∞ design.

Then, the realization of the transfer matrix P is taken to be of the form:

$$P(s) = \left[\begin{array}{c|cc} A & B_1 & B_2 \\ \hline C_1 & D_{11} & D_{12} \\ C_2 & D_{21} & 0 \end{array} \right] \quad (2.12)$$

In addition, the following assumptions are employed:

A1) (A, B_2) is stabilizable and (C_2, A) is detectable;

A2) $\begin{bmatrix} A - j\omega I & B_2 \\ C_1 & D_{12} \end{bmatrix}$ has full column rank $\forall \omega \in \mathbb{R}$;

A3) $\begin{bmatrix} A - j\omega I & B_1 \\ C_2 & D_{21} \end{bmatrix}$ has full row rank $\forall \omega \in \mathbb{R}$;

A4) $D_{12}^* D_{12} = I$ and $D_{21} D_{21}^* = I$.

Assumption (A1) is necessary for the existence of stabilizing controllers. Furthermore, assumptions (A2) and (A3) are needed for a technical reason for guarantee of the two Hamiltonian matrices. In addition, assumption (A4) are made to simplify the exposition. In fact, only the non-singularity of the matrices $D_{12}^*D_{12}$ and $D_{21}D_{21}^*$ is required. For the general matrices D_{11}, D_{12}, D_{21} and D_{22} , a solution is found in [32].

The solution, which is stated in Theorem 1, involves two Hamiltonian matrices

$$H_x := \begin{bmatrix} A & 0 \\ -C_1^* C_1 & -A^* \end{bmatrix} - \begin{bmatrix} B \\ -C_1^* D_{1\bullet} \end{bmatrix} R^{-1} \begin{bmatrix} D_{1\bullet}^* C_1 & B^* \end{bmatrix}. \quad (2.13)$$

$$J_y := \begin{bmatrix} A^* & 0 \\ -B_1 B_1^* & -A \end{bmatrix} - \begin{bmatrix} C^* \\ -B_1 D_{\bullet 1}^* \end{bmatrix} \tilde{R}^{-1} \begin{bmatrix} D_{\bullet 1} B_1^* & C \end{bmatrix}. \quad (2.14)$$

where,

$$R := D_{1\bullet}^* D_{1\bullet} - \begin{bmatrix} \gamma^2 I & 0 \\ 0 & 0 \end{bmatrix}, \quad (2.15)$$

$$\tilde{R} := D_{\bullet 1} D_{\bullet 1}^* - \begin{bmatrix} \gamma^2 I & 0 \\ 0 & 0 \end{bmatrix}, \quad (2.16)$$

and

$$D_{1\bullet} := \begin{bmatrix} D_{11} & D_{12} \end{bmatrix}, \quad (2.17)$$

$$D_{\bullet 1} := \begin{bmatrix} D_{11} \\ D_{21} \end{bmatrix}. \quad (2.18)$$

The stable solutions X and Y of the Riccati equations are obtained

$$X := Ric(H_x) \text{ and } Y := Ric(J_y) \quad (2.19)$$

and the *state feedback* and *output injection* matrices F and L are determined as

$$F := \begin{bmatrix} F_{1\bullet} \\ F_{2\bullet} \end{bmatrix} := -R^{-1} [D_{1\bullet}^* C_1 + B^* X], \quad (2.20)$$

$$L := \begin{bmatrix} L_{1\bullet} & L_{2\bullet} \end{bmatrix} := -[B_1 D_{\bullet 1}^* + Y C^*] \tilde{R}^{-1}, \quad (2.21)$$

with the partition D , $F_{1\bullet}$, and $L_{1\bullet}$:

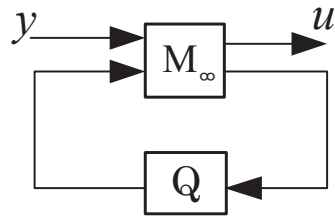
$$\left[\begin{array}{c|c} & F' \\ \hline L' & D \end{array} \right] = \left[\begin{array}{c|ccc} & F_{11\bullet}^* & F_{12\bullet}^* & F_{2\bullet}^* \\ \hline L_{11\bullet}^* & D_{1111} & D_{1112} & 0 \\ L_{12\bullet}^* & D_{1121} & D_{1122} & I \\ L_{2\bullet}^* & 0 & I & 0 \end{array} \right] \quad (2.22)$$

Theorem 1. Assume P fulfills the assumptions (A1) to (A4). Then there is a stabilizing controller K , such that $\|\mathcal{F}_l(G, K)\|_\infty \leq \gamma$ if and only if:

- (i) $\gamma > \max \bar{\sigma}[D_{1111} \ D_{1112}], \bar{\sigma}[D_{1111}^* \ D_{1121}^*]$,
- (ii) $H_x \in \text{dom}(\text{Ric})$ and $X \geq 0$,
- (iii) $J_y \in \text{dom}(\text{Ric})$ and $Y \geq 0$,
- (iv) $\sigma(XY) < \gamma^2$

Using the notation \mathcal{F}_l for the lower fractional transformation, stabilizing controllers $K(s)$ is given by $K = \mathcal{F}_l(M_\infty, Q)$ for arbitrary $Q \in RH_\infty$ such that $\|Q\|_\infty \leq \gamma$, where

$$M_\infty = \left[\begin{array}{c|cc} \hat{A} & \hat{B}_1 & \hat{B}_2 \\ \hline \hat{C}_1 & \hat{D}_{11} & \hat{D}_{12} \\ \hat{C}_2 & \hat{D}_{21} & 0 \end{array} \right]$$



and the parameters are given as:

$$\hat{D}_{11} = -D_{1121} D_{1111}^* (\gamma^2 I - D_{1111} D_{1111}^*)^{-1} D_{1112} - D_{1122}, \quad (2.23)$$

\hat{D}_{12} and \hat{D}_{21} fulfill:

$$\hat{D}_{12} \hat{D}_{12}^* = I - D_{1121} (\gamma^2 I - D_{1111}^* D_{1111})^{-1} D_{1121}^*, \quad (2.24)$$

$$\hat{D}_{21}^* \hat{D}_{21} = I - D_{1112}^* (\gamma^2 I - D_{1111} D_{1111}^*)^{-1} D_{1112}, \quad (2.25)$$

and

$$\hat{B}_2 = Z_\infty (B_2 + L_{12\bullet}) \hat{D}_{12}, \quad (2.26)$$

$$\hat{C}_2 = -\hat{D}_{21} (C_2 + F_{12\bullet}), \quad (2.27)$$

$$\hat{B}_1 = -Z_\infty L_{2\bullet} + \hat{B}_2 \hat{D}_{12}^{-1} \hat{D}_{11}, \quad (2.28)$$

$$\hat{C}_1 = F_{2\bullet} + \hat{D}_{11} \hat{D}_{21}^{-1} \hat{C}_2, \quad (2.29)$$

$$\hat{A} = A + BF + \hat{B}_1 \hat{D}_{21}^{-1} \hat{C}_2. \quad (2.30)$$

Finally,

$$Z_\infty = (I - \gamma^{-2} Y X)^{-1}. \quad (2.31)$$

In this thesis, we use Matlab/Simulink for H_∞ computations for LTI plants. In particular, we apply the function **hinfsyn**, which computes a stabilizing H_∞ optimal controller K for a partitioned plant P .

CHAPTER 3

CACC DESIGN FOR HETEROGENEOUS VEHICLES

In this chapter, the CACC design is developed for heterogeneous vehicles, such that a platoon of vehicles with different dynamics achieves string-stability and safe vehicle-following.

3.1 Longitudinal Vehicle Dynamics

Vehicles (cars, trucks, buses) represent interesting and complex mechanical systems with nonlinear characteristics that require accurate analysis [26, 33]. The model dynamics have to capture complex aspects of vehicle dynamics such as aerodynamics, geometry, mass, motion and tire specifications of each vehicle. Therefore, many studies have been developed in order to understand the behavior of both light and heavy vehicles. Moreover, these studies are based on using exact linearization methods to linearize the input-to-output behavior of each vehicle in the platoon [34, 35, 36, 33]. In order to control the longitudinal position of platoon vehicles, it is considered that the speed of each vehicle is controlled to a desired value using the throttle input [26]. The longitudinal control system architecture for the cruise control vehicle will be designed to be hierarchical, with an upper level controller and a lower level controller as shown in Figure 12.

The upper level controller determines the desired acceleration for the vehicle. The lower level controller determines the throttle input required to track the desired acceleration. A detailed vehicle dynamics model are for the lower controller in calculating the real-time throttle input required to track the desired acceleration [26]. For the i -th vehicle in the string, the high-level mode is given by the following linear third-order

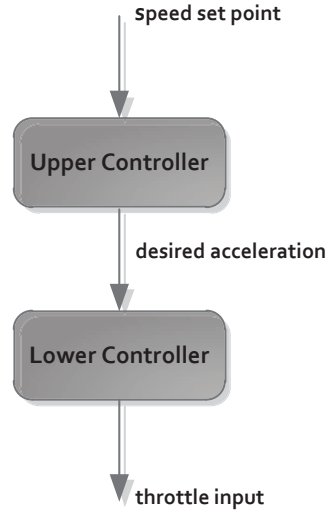


Figure 12: Structure of cruise control system.

state-space representation of the longitudinal dynamics:

$$\begin{bmatrix} \dot{q}_i(t) \\ \dot{v}_i(t) \\ \dot{a}_i \end{bmatrix} = \begin{bmatrix} v_{i-1}(t) - v_i(t) \\ a_i(t) \\ -a_i(t)/\tau_i + u_i(t - \theta_i)/\tau_i \end{bmatrix} \quad (3.1)$$

where q_i , v_i and a_i are respectively the absolute position, velocity and acceleration. τ_i represents the time constant of the internal dynamic vehicle, θ_i is a plant delay and u_i is the control input of the i -th vehicle. This model is widely used in the literature as a basis of analysis [15, 16, 34, 35]. Equivalently, by using Laplace transforms, $\mathcal{L}(q_i(t)) = Q_i(s)$ and $\mathcal{L}(u_i(t)) = U_i(s)$, the vehicle model can be represented by the following transfer function as in (3.2):

$$G_i(s) = \frac{e^{-\theta_i s}}{(1 + s \tau_i) s^2} = \frac{Q_i(s)}{U_i(s)}. \quad (3.2)$$

The actual acceleration of the vehicle is assumed to track the desired acceleration with a time constant τ_i , so according to the specific value τ_i , we can measure the different types of vehicle driveline dynamics. For instance, the τ_i value of a Volvo S60 car is

about 0.45 [37], while the literature uses $0.9 \leq \tau_i \leq 1.4$ for heavy vehicles, considering that the best condition for heavy vehicle is taken as $\tau_i \approx 0.9$ according to [38]. For more information about computing the τ_i value, [26] can be consulted.

3.2 Modified Block Diagram

The CACC controller from the existing literature [15] is suitable for homogeneous strings. In particular, the design uses the fact that:

$$\Gamma(s) = \frac{U_i(s)}{U_{i-1}(s)} = \frac{V_i(s)}{V_{i-1}(s)}. \quad (3.3)$$

That is, although the relation $\frac{V_i(s)}{V_{i-1}(s)}$ is relevant in practice¹ [39], it is possible to design the CACC controller K using the ratio $\frac{U_i(s)}{U_{i-1}(s)}$ according to the block diagram in Figure 13.

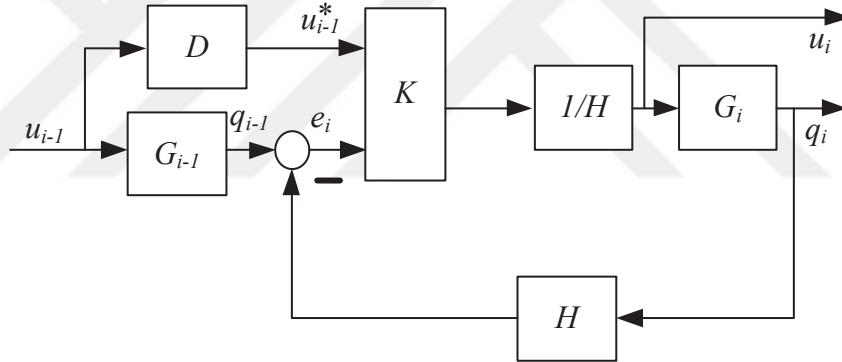


Figure 13: Feedback loop for CACC.

The vehicle i has the transfer function

$$G_i(s) = \frac{1}{(1 + s \tau_i) s^2} = \frac{Q_i(s)}{U_i(s)} \quad (3.4)$$

¹It is desired that velocity fluctuations of vehicle $i - 1$ are attenuated by vehicle i .

and its predecessor vehicle has the same transfer function with different value of time constant τ

$$G_{i-1}(s) = \frac{1}{(1 + s \tau_{i-1}) s^2} = \frac{Q_{i-1}(s)}{U_{i-1}(s)}. \quad (3.5)$$

This is no longer true in the case of *heterogeneous vehicles* where generally $\tau_{i-1} \neq \tau_i$. In order to evaluate the ratio $\frac{V_i(s)}{V_{i-1}(s)}$, assume

$$V_{i-1}(s) = s Q_{i-1}(s) = \frac{1}{1 + s \tau_{i-1} s} U_{i-1}(s) \quad (3.6)$$

and;

$$V_i(s) = s Q_i(s) = \frac{1}{1 + s \tau_i s} U_i(s) \quad (3.7)$$

from (3.2). Together, it holds that;

$$\begin{aligned} \frac{V_i(s)}{V_{i-1}(s)} &= \frac{1}{1 + s \tau_i s} \frac{1}{s} U_i(s) \left(\frac{1}{1 + s \tau_{i-1} s} \frac{1}{s} U_{i-1}(s) \right)^{-1} \\ &= \frac{1 + s \tau_{i-1}}{1 + s \tau_i} \frac{U_i(s)}{U_{i-1}(s)} = \frac{G_i(s)}{G_{i-1}(s)} \Gamma(s) =: \Gamma_i(s). \end{aligned}$$

Therefore,

$$\Gamma(s)_{for heter. veh.} := \Gamma_i(s) = \frac{G_i}{G_{i-1}} \frac{DK_{ff} + G_{i-1}K_{fb}}{H(1 + G_iK_{fb})}. \quad (3.8)$$

In order to obtain strict string stability in the developed setting, it is required by (2.5) that

$$\|\Gamma_i(s)\|_{\infty} \leq 1 \quad (3.9)$$

for all vehicles i .

3.3 String Stability Bounds

Regarding (3.9), it has to be noted that τ_i is known when designing the controller K_i for vehicle i . Nevertheless, the dynamics of the predecessor vehicle $i - 1$ (represented

by τ_{i-1}) are not known. Vehicle i can have different predecessor vehicles depending on the traffic situation. That is, it is essential for each vehicle i that (3.9) is fulfilled for a sufficiently large range of values τ_{i-1} such that vehicle i can follow different predecessor vehicles without violating strict string stability and without changing the controller.

In this section, we develop an original method for analyzing the range of suitable values for τ_{i-1} . To this end, we assume that a controller K_i has been computed for vehicle i . It is then desired to find out which time constants τ_{i-1} for vehicle $i-1$ are suitable such that $\|\Gamma_i(s)\|_\infty \leq 1$. We next propose two bi-partition algorithms in order to determine an upper bound τ_{i-1}^{\max} (Algorithm 1) and a lower bound τ_{i-1}^{\min} for τ_{i-1} (Algorithm 2). Both algorithms are developed using a particular assumption that can be verified for the transfer function $\Gamma_{i-1}(s)$ in (3.8): let τ_{i-1}, τ'_{i-1} be time constants such that $\|\Gamma_{i-1}\|_\infty \leq 1$. Then, it holds for all τ''_{i-1} between τ_{i-1} and τ'_{i-1} that $\|\Gamma_{i-1}\|_\infty \leq 1$.

Algorithm 1 bisects the difference between an upper value τ_u^{\max} and a lower value τ_l^{\max} until they are sufficiently close (threshold value ε). Hereby, it is initially required that $\|\Gamma_i(s)\|_\infty \leq 1$ for $\tau_{i-1} = \tau_{l,0}^{\max}$ and $\|\Gamma_i(s)\|_\infty > 1$ for $\tau_{i-1} = \tau_{u,0}^{\max}$.² The result τ_1^{\max} gives an upper bound for τ_{i-1} (slowest possible predecessor vehicle) to obtain strict string stability. In analogy to Algorithm 1, Algorithm 2 determines a lower bound on

Algorithm 1 Bi-partition algorithm for computing τ_{i-1}^{\max}

```

1: input:  $\tau_{u,0}^{\max}, \tau_{l,0}^{\max}, \varepsilon$ 
2: output:  $\tau_{i-1}^{\max}$ 
3:  $\tau_u^{\max} = \tau_{u,0}^{\max}, \tau_l^{\max} = \tau_{l,0}^{\max}$ 
4: while  $\tau_u^{\max} - \tau_l^{\max} > \varepsilon$  do
5:    $\tau_{i-1} := \frac{\tau_l^{\max} + \tau_u^{\max}}{2}$ 
6:   if  $\|\Gamma_i(s)\|_\infty > 1$  then
7:      $\tau_u^{\max} := \tau_{i-1}$ 
8:   else
9:      $\tau_l^{\max} := \tau_{i-1}$ 
10:  end if
11:
12: end while
13:  $\tau_i^{\max} = \tau_l^{\max}$ 

```

τ_{i-1} (fastest possible predecessor) for strict string stability. Initially, it is required that

² $\tau_{l,0}^{\max}$ can be obtained from the controller design and $\tau_{u,0}^{\max} \gg \tau_i$ can be chosen manually.

$\|\Gamma_i(s)\|_\infty \leq 1$ for $\tau_{u,0}^{\min}$ and $\|\Gamma_i(s)\|_\infty > 1$ for $\tau_{l,0}^{\min}$. Based on Algorithm 1 and 2, it is

Algorithm 2 Bi-partition algorithm for computing τ_{i-1}^{\min}

```

1: input:  $\tau_{u,0}^{\min}, \tau_{l,0}^{\min}, \varepsilon$ 
2: output:  $\tau_{i-1}^{\min}$ 
3:  $\tau_u^{\min} = \tau_{u,0}^{\min}, \tau_l^{\min} = \tau_{l,0}^{\min}$ 
4: while  $\tau_u^{\min} - \tau_l^{\min} > \varepsilon$  do
5:    $\tau_{i-1} = \frac{\tau_l^{\min} + \tau_u^{\min}}{2}$ 
6:   if  $\|\Gamma_i(s)\|_\infty > 1$  then
7:      $\tau_l^{\min} = \tau_{i-1}$ 
8:   else
9:      $\tau_u^{\min} = \tau_{i-1}$ 
10:  end if
11:
12: end while
13:  $\tau_{i-1}^{\min} = \tau_u^{\min}$ 

```

possible to determine a range of values for τ_{i-1} in order to achieve strict string stability. Accordingly, we obtain the following result.

Proposition 1. *Let $G_i(s)$ be a plant and $K_i(s)$ be a controller. Assume that τ_{i-1}^{\max} and τ_{i-1}^{\min} are computed with Algorithm 1 and 2, respectively, whereby $\tau_{l,0}^{\max} \leq \tau_{u,0}^{\min}$. Then, $\|\Gamma_i(s)\|_\infty \leq 1$ for all $\tau_{i-1}^{\min} \leq \tau_{i-1} \leq \tau_{i-1}^{\max}$.*

According to Algorithm 1, strict string stability is fulfilled for $\tau_{l,0}^{\max} \leq \tau_{i-1} \leq \tau_{i-1}^{\max}$. Likewise, Algorithm 2 implies that strict string stability is fulfilled for $\tau_{i-1}^{\min} \leq \tau_{i-1} \leq \tau_{u,0}^{\min}$. Since $\tau_{l,0}^{\max} \leq \tau_{u,0}^{\min}$, this directly implies that following-vehicle i is valid to follow predecessor vehicle $i - 1$ with range of vehicles $\tau_{i-1}^{\min} \leq \tau_{i-1} \leq \tau_{i-1}^{\max}$.

3.4 Controller Design Method for Heterogeneous Vehicles

The previous section analyses the possible dynamics of predecessors of a vehicle i such that strict string stability is guaranteed under the assumption that K_i is already determined. In this section, we propose the first method in the literature for designing K_i under the assumption of heterogeneous strings. To this end, we recall that K_i must be found such that (3.9) is fulfilled for each vehicle i and for all possible predecessor vehicles $i - 1$. We use H_∞ -design with the following block diagram. Here, W is a weighting transfer function.

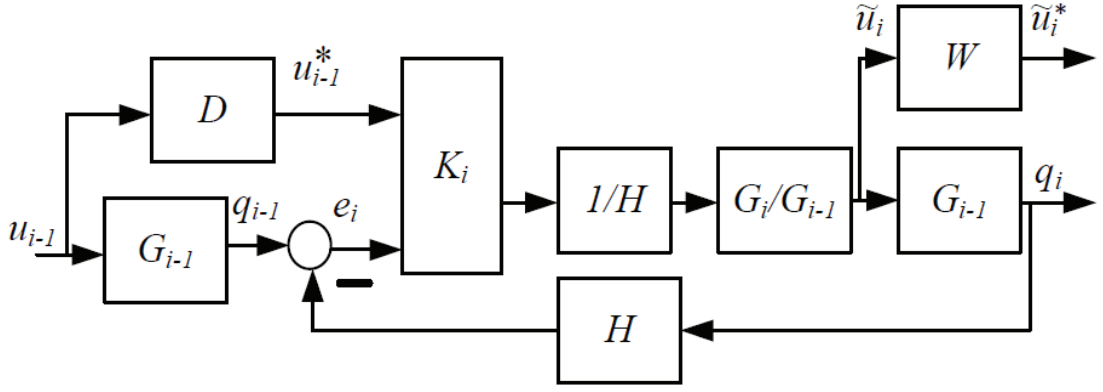


Figure 14: Feedback loop for CACC with heterogeneous vehicles.

We note that the block diagram is arranged such that $\frac{\tilde{U}_i(s)}{U_{i-1}(s)} = \Gamma_i(s)$ in (3.8). The modified sensitivity is

$$S_i(s) = \frac{E_i(s)}{U_{i-1}(s)} = \frac{G_{i-1} + DK_{i,ff}G_i}{1 + K_{i,fb}G_i}. \quad (3.10)$$

We propose to compute K_i for each vehicle i such that

$$\min_{K_i} \left\| \begin{array}{c} \Gamma_i(s)W \\ S_i(s) \end{array} \right\| \leq 1 \quad (3.11)$$

and choose W such that string stability is achieved for a sufficient range of τ_{i-1} . To this end, we use the LFT in Figure 15 with the matrix P_i evaluated from Figure 14. In this design, G_{i-1}^{\min} denotes the vehicle model with the smallest possible value of $\tau_{i-1} = \tau^{\min}$.

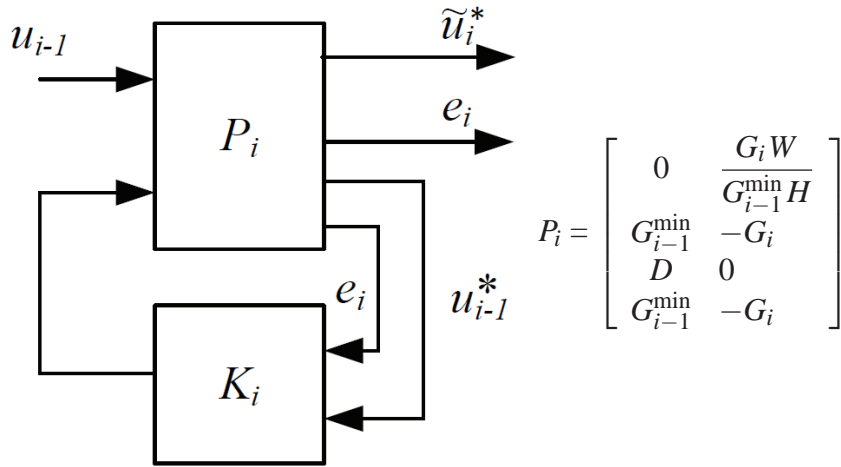


Figure 15: H_∞ control loop for heterogeneous vehicles.

The described design method computes the controller K_i to be implemented on vehicle i . That is, the dynamics of vehicle i (time constant τ_i) is known. Nevertheless, the dynamics of the predecessor vehicle $i - 1$ is uncertain. The idea of the design method is to assume the fastest vehicle ($\tau_{i-1} = \tau^{\min}$) as predecessor $i - 1$. If the design achieves strict string stability for $\tau_{i-1} = \tau^{\min}$, it is expected that the design is also successful for values of $\tau_{i-1} \geq \tau^{\min}$. In addition, the weighting transfer function W is used to further increase the range of τ_{i-1} . Examples are provided in the next section.

3.5 Simulation Study For Heterogeneous

3.5.1 CACC Controller Computation

In this section, computations and simulations for heterogeneous vehicle strings are performed. In first example Figure 16, we assume deviations of about 0.3 from that average value of $\tau_i = 0.4$ such that we are interested in the range $0.1 \leq \tau_i \leq 0.7$ with $\tau^{\min} = 0.1$. As the first step of our evaluation, we use (3.11) to determine K_i for the different vehicle parameter values $\tau_i = 0.1, 0.2, 0.3, 0.4, 0.5, 0.6, 0.7$. Table 1 shows the respective weighting transfer function and the upper and lower bounds for string stability according to Algorithm 1 and 2. It can be seen that string stability is achieved for the whole range of vehicles with $\tau_{i-1}^{\min} \leq 0.1 \leq \tau_{i-1} \leq 0.7 \leq \tau_{i-1}^{\max}$. Hereby, we note that the choice of the weighting transfer function W is tuned manually and the plant delay θ and communication delay ϕ are assumed to be zero in this initial research.

τ_i	W	τ_{i-1}^{\min}	τ_{i-1}^{\max}	τ_i	W	τ_{i-1}^{\min}	τ_{i-1}^{\max}
0.1	$\frac{1+.9s}{1+.09s}$	0	0.758	0.5	$\frac{1+.85s}{1+.12s}$	0	0.723
0.2	$\frac{1+.9s}{1+.09s}$	0	0.758	0.6	$\frac{1+.85s}{1+.12s}$	0	0.723
0.3	$\frac{1+.85s}{1+.12s}$	0	0.723	0.7	$\frac{1+.85s}{1+.12s}$	0	0.722
0.4	$\frac{1+.85s}{1+.12s}$	0	0.723				

Table 1: Parameters for the CACC controller design for first example.

In the second example in Figure 18, we assume deviations of about 0.4 to the average value of $\tau_i = 0.5$ such that we are interested in the range $0.1 \leq \tau_i \leq 0.9$ with $\tau^{\min} = 0.1$. K is computed according to (3.11) for different τ values as shown in Table 2, which are fulfilled (3.9) by using Algorithm 1 and 2.

τ_i	W	τ_{i-1}^{\min}	τ_{i-1}^{\max}	τ_i	W	τ_{i-1}^{\min}	τ_{i-1}^{\max}
0.1	$\frac{1+s}{1+.4s}$	0	1	0.6	$\frac{1+1.3s}{1+.06s}$	0	1
0.2	$\frac{1+1.3s}{1+.4s}$	0	.97	0.7	$\frac{1+1.2s}{1+.3s}$	0	.96
0.3	$\frac{1+1.3s}{1+.4s}$.06	1	0.8	$\frac{1+1.2s}{1+.2s}$	0	1
0.4	$\frac{1+1.3s}{1+.05s}$	0	.98	0.9	$\frac{1+1.3s}{1+.3s}$	0	.92
0.5	$\frac{1+1.3s}{1+.05s}$	0	1				

Table 2: Parameters for the CACC controller design for second example.

3.5.2 Simulation with Heterogeneous Vehicles

We now evaluate the controller design in the previous section by simulations in Matlab/Simulink. To this end, we consider the same heterogeneous vehicle string as in Section 2.5. In the simulation, the controller K_i for the respective time constant τ_i as computed in Section 3.5.1 is used for each vehicle.

The simulation result is shown in Figure 16 and 18. From the position signal for each example, it is readily observed that the vehicles follow their predecessor at a safe distance and the velocity signals confirm that strict string stability is achieved in the proposed design. The velocity disturbance of the leader vehicle 1 is indeed attenuated along the heterogeneous vehicle string. In addition, we zoom in on the interesting part of the simulation in Figure 16 for the velocity and acceleration signal in order to study the heterogeneous vehicle behavior in platoon. Figure 17 shows that vehicle 2 (which is represented by the green line) is following its predecessor vehicle 1 (which is represented by the blue line) fast since vehicle 2 has faster dynamics than vehicle 1. At the same time, string-stability is fulfilled. In contrast, vehicle 3 (which is represented by the red line) is following its predecessor vehicle (green line) slowly since vehicle 3 has slower dynamics than vehicle 2. Nevertheless, string-stability is still fulfilled. Finally, each line shows that the vehicles are following their respective predecessor vehicle in a safe distance and without violating string-stability. This is independent of whether fast vehicles (small τ) follow slow vehicles (large τ) or vice versa.

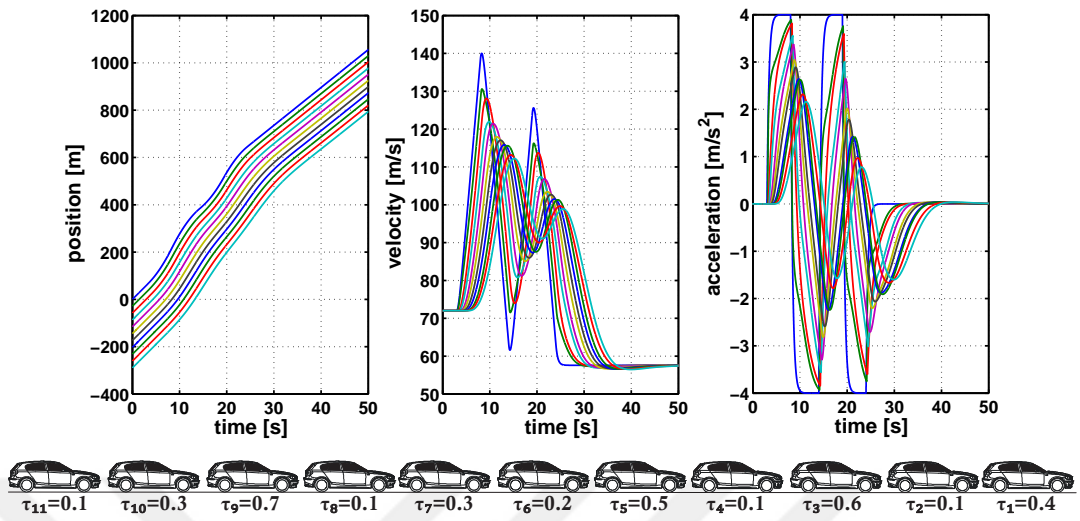


Figure 16: CACC simulation with heterogeneous vehicles and strict string stability for first example.

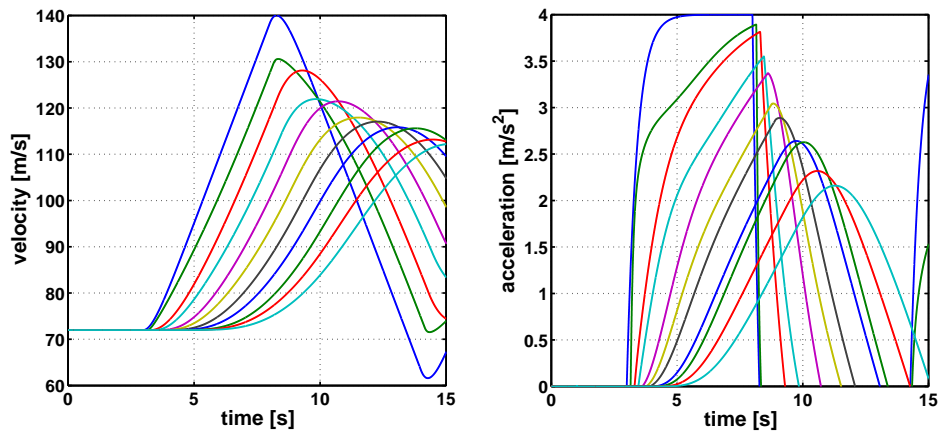


Figure 17: Zoom in figure for velocity and acceleration of first example.

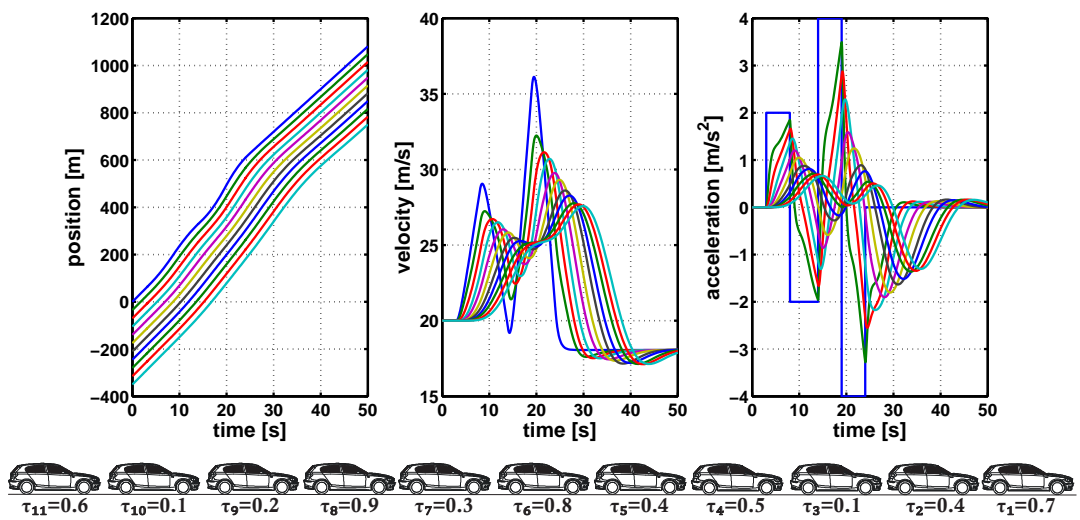


Figure 18: CACC simulation with heterogeneous vehicles and strict string stability for second example.

CHAPTER 4

CACC DESIGN WITH TIME-DELAY

The objective of the chapter is to find a solution for CACC design with time delay in order to obtain string stability for realizing safe vehicle following at small inter-vehicle spacing.

4.1 Introduction

Time-delay exists in many real-world engineering systems such as the control systems, communication networks, intelligent transportation systems (ITS), hydraulic systems, heating systems and so on [28]. It has been realized that time delay predominantly is a source for instability of system or poor performance of control systems [40]. For this reason, the presence of delay makes system analysis and control design complicated [28, 41]. Therefore, the stability analysis and robust control of time delay systems are of theoretical and practical importance [42]. Delay is defined as a unit that causes a

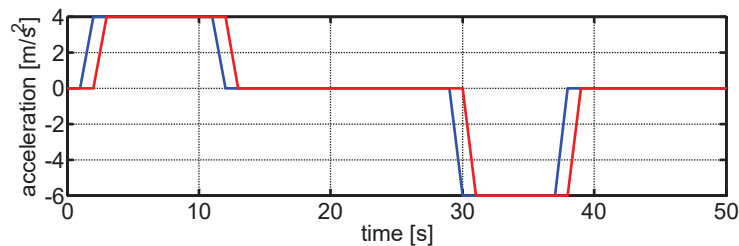


Figure 19: System with delay.

time-shift in the signal. An ideal delay is a delay system which has no effect on the signal characteristics at all [41, 43, 40], for example delayed acceleration signal as shown in Figure 19.

4.2 CACC Model with Delay

The general form of a CACC model includes 2 delays [15], as shown in Figure 20.

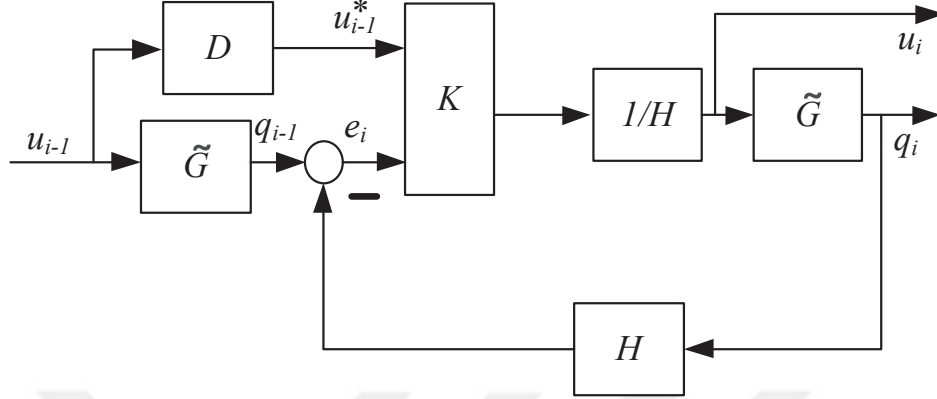


Figure 20: CACC model with delay.

$D = e^{-s\theta}$ refers to the communication delay of data which is transmitted by wireless communication from the predecessor vehicle. Communication delay undertaken in vehicle platoons is widely dependent on the network architecture adopted [42]. On the other hand, the vehicle dynamics with delay is described in the Laplace domain by the transfer function $\tilde{G}(s)$:

$$\tilde{G}_i(s) = \frac{e^{-\phi s}}{(1 + s\tau_i)s^2} = \frac{Q_i(s)}{U_i(s)}, \quad (4.1)$$

where $\tilde{G}_i(s) = e^{-\phi s}G(s)$ and $G(s)$ is the rational part of the dynamic plant model, τ is a time constant and ϕ is a time delay of internal vehicle dynamic. U_i is the vehicle input (*desired acceleration*) and the position Q_i is the output (*desired distance*). This chapter is focused on finding a solution for the H_∞ control design for CACC with delay.

4.3 Controller Realizations

4.3.1 Rational controller

In previous chapters, CACC is designed by H_∞ control that does not consider delays to achieve the string stability conditions [chapter 2, 3]. The basic feedback loop for the

CACC is shown in Figure 20. K is the controller transfer matrix which can be written as

$$K = \begin{bmatrix} K_{ff} & K_{fb} \end{bmatrix}. \quad (4.2)$$

K_{ff} is a feedforward controller and K_{fb} is a feedback controller transfer function. Assuming that all vehicle dynamics are similar, the transfer function Γ is formed from Figure 20, for all vehicles i :

$$\Gamma(s) := \Gamma_i(s) = \frac{U_i(s)}{U_{i-1}(s)} = \frac{DK_{ff} + G_i K_{fb}}{H(1 + G_i K_{fb})}. \quad (4.3)$$

For a rational controller design, θ and ϕ are assumed to be zero. The platoon vehicles achieve strict string stability if and only if the Γ of all vehicles i is:

$$\|\Gamma(s)\|_\infty \leq 1. \quad (4.4)$$

In order to fulfill (4.4) and at the same time minimize the position error $e_i(t)$, the H_∞ control problem is formulated as;

$$\min_K \left\| \begin{bmatrix} \Gamma(s) \\ S(s) \end{bmatrix} \right\|_\infty \leq 1. \quad (4.5)$$

Here, $S(s)$ is the closed-loop sensitivity corresponding to vehicle i as shown in (4.6).

$$S(s) = \frac{E_i(s)}{U_{i-1}(s)} = \frac{G(1 - DK_{ff})}{1 + GK_{fb}}. \quad (4.6)$$

The method in chapter 2 is proposed to design controller K (which considers that the delays are zero) under the requirement of string stability. As a consequence, the lower fractional transformation (LFT) with the corresponding matrix P is evaluated from Figure 20, as shown in Figure 48.

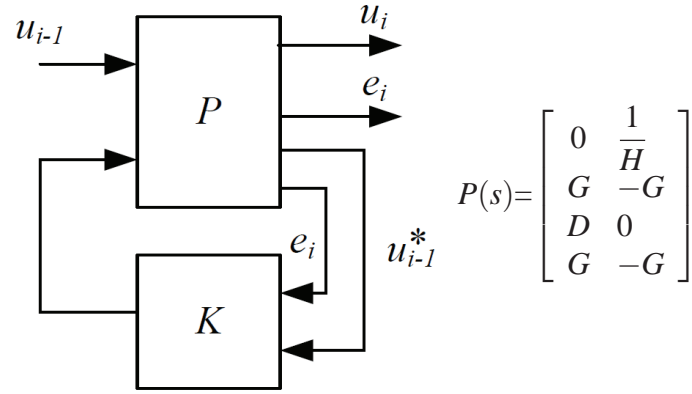


Figure 21: H_∞ design for CACC.

4.3.2 Modified CACC with Predictor

One of the possible approaches to control processes for time-delay with stable closed-loop, high performance and stability, is the usage of a controller with predictor as seen in the literature [28, 44, 45, 46, 47]. Moreover, this predictor provides useful and practical guidelines for the development of a systematic robust design method for system with delay.

In the new proposal of CACC model, a predictor is added to the closed-loop as shown in Figure 22. Particularly, this model with predictor is developed to design H_∞ control for CACC with delays under the requirement of string stability.

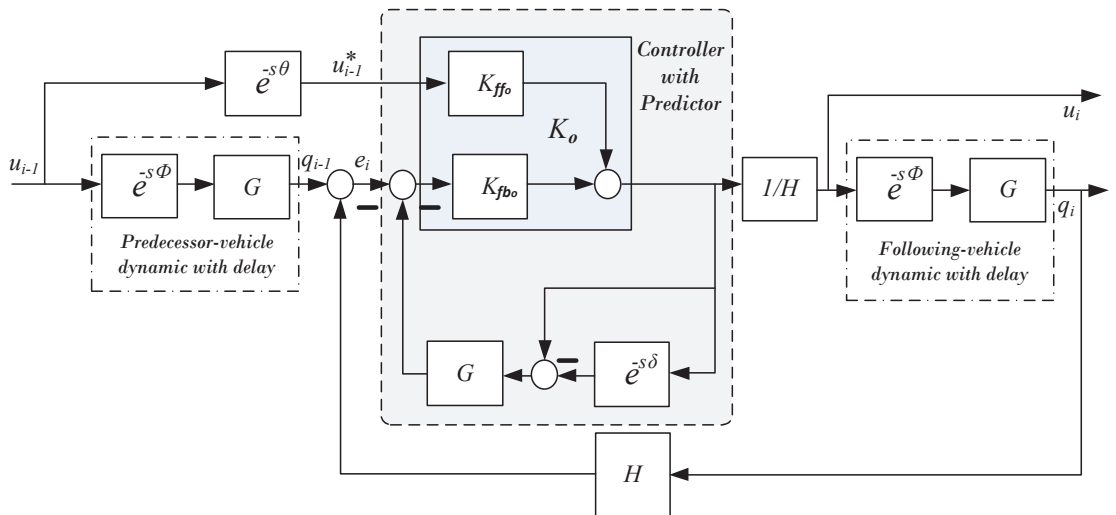


Figure 22: CACC model with predictor.

From Figure 22, the plant $\tilde{G}(s) = e^{-s\phi} G(s)$ is a dynamic vehicle system with delay ϕ , θ is a communication delay and δ is assumed as a mutual delay between communication and dynamic delays. The predictor helps to shift the delay outside the feedback loop and preserving stability of the closed-loop. As a consequence, the control design and system analysis are considerably simplified. This is realized by introducing local feedback to the main controller $K_o(s)$. Hence, a main controller combined with a predictor forms the overall controller $K(s)$ of the system as shown in (4.7).

$$K = \left[K_{ffo} \quad \frac{K_{fb_o}}{1 + K_{fb_o} G(1 - e^{-s\delta})} \right]. \quad (4.7)$$

4.3.3 Modified String Stability for CACC with Predictor

The definition of the string stability of a platoon of vehicles is assumed as seen in previous chapters which is obtained from a linear system representation;

$$\Gamma_i(s) = \frac{U_i(s)}{U_{i-1}(s)}. \quad (4.8)$$

From Figure 22, the transfer function $\Gamma(s)$ with predictor is written for each vehicle i as

$$\Gamma(s) := \Gamma_i(s) = \frac{U_i(s)}{U_{i-1}(s)} = \frac{e^{-s\theta_i} K_{ffo} + e^{-s\phi_i} G_i K_{fb}}{H(1 + e^{-s\phi_i} G_i K_{fb})}. \quad (4.9)$$

Here, the feedback controller K_{fb} represents the main controller K_{fb_o} with predictor loop as shown in (4.10);

$$K_{fb}(s) = \frac{K_{fb_o}}{1 + K_{fb_o} G(1 - e^{-s\delta})}. \quad (4.10)$$

To this end, strict string stability is achieved if and only if all vehicles i fulfill

$$\|\Gamma_i(s)\|_\infty \leq 1. \quad (4.11)$$

In order to achieve (4.11), we need to compute the infinity norm of $\|\Gamma\|_\infty$, which includes an exponential term (time delay). According to this reason, the computation of the $\|\Gamma\|_\infty$ is performed by utilizing *bode*, or *nyquist* plot since the considered system

has a single input and single output.

4.4 Padé-Approximation

The transfer function of delay e^{-sT} is irrational. Therefore, in some conditions, it is possible to substitute e^{-sT} with an approximation in form of a rational transfer function. The most common approximation is the Padé-approximation which is based on a minimization of the truncation errors in a finite series expansion of e^{-sT} [15, 48, 49, 50, 51, 52] as shown in the form of:

$$e^{-sT} \approx \frac{1 - k_1s + k_2s^2 + \dots \pm k_ns^n}{1 + k_1s + k_2s^2 + \dots + k_ns^n}. \quad (4.12)$$

where n is the order of the approximation. The coefficients k_i are functions of n .

4.4.1 Controller Design by Padé-Approximation

It is assumed that the lower fractional transformation (LFT) with the corresponding matrix P includes delays as shown in a Section 4.3.1. In addition, each scenario of delay in the CACC is converted to rational transfer function by Padé-approximation as shown in the Table 3. To this end, the computation of H_∞ control is identical to Section 2.6. Furthermore, high and low orders¹ of the Padé-approximation are utilized in the controller design.

Delay value	Second-order	Fifth-order
$e^{-s0.1} \approx$	$\frac{s^2-60s+1200}{s^2+60s+1200}$	$\frac{-s^5+300s^4-42000s^3+3.36 \cdot 10^6s^2-1.512 \cdot 10^8s+3.024 \cdot 10^9}{s^5+300s^4+42000s^3+3.36 \cdot 10^6s^2+1.512 \cdot 10^8s+3.024 \cdot 10^9}$
$e^{-s0.3} \approx$	$\frac{s^2-20s+133.3}{s^2+20s+133.3}$	$\frac{-s^5+100s^4-4667s^3+1.244 \cdot 10^5s^2-1.867 \cdot 10^6s+1.244 \cdot 10^7}{s^5+100s^4+4667s^3+1.244 \cdot 10^5s^2+1.867 \cdot 10^6s+1.244 \cdot 10^7}$
$e^{-s0.5} \approx$	$\frac{s^2-12s+48}{s^2+12s+48}$	$\frac{-s^5+60s^4-1680s^3+2.688 \cdot 10^4s^2-2.419 \cdot 10^5s+9.677 \cdot 10^5}{s^5+60s^4+1680s^3+2.688 \cdot 10^4s^2+2.419 \cdot 10^5s+9.677 \cdot 10^5}$

Table 3: Some converted delays by Padé-approximation.

4.4.2 Simulation and Experimental Results

Experiments show the impact of the Padé-approximation on string stability for the CACC design when ϕ_i and θ_i are same. These simulations are executed with a string of

¹Increasing order of the Padé-approximation, makes the controller more complex due to high order of transfer functions

6 vehicles by MATLAB/SIMULINK as shown in Figure 23. where, $\tau_i = 0.4$ is consid-

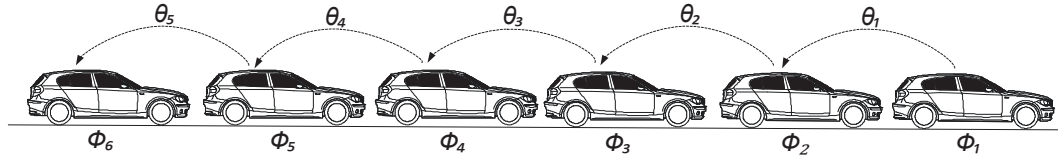


Figure 23: String of six vehicles .

ered for each vehicle and headway time is 0.7. The controllers K are computed by using the second-order and fifth-order of Padé-approximation for each scenario of delay as shown in Table 3. In the first simulation, the dynamic and communication delays are assumed to be 0.1s. In the second simulation, the delays are assumed to be 0.3s. In the last simulation, the delays are assumed to be 0.5s. The leader vehicle is provided with the input signal in Figure 24. That is, sharp accelerations of 2m/s^2 and -4m/s^2 are given in order to study a difficult vehicle following scenario.

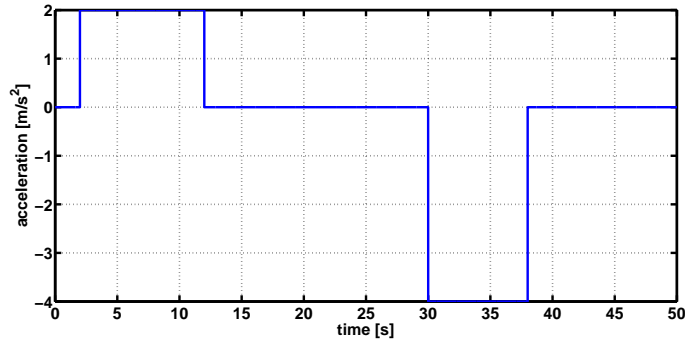


Figure 24: Acceleration input.

The simulation results are shown in Figures 25, 27 and 29 for design by second-order Padé-approximation and Figures 26, 28 and 30 for design by fifth-order Padé-approximation. It can be seen from the vehicles positions that each vehicle follows its predecessor at a safe distance, and smoothly tracks the leader acceleration and velocity while maintaining small fluctuations around the target distance. In addition, the velocity and acceleration plot suggest that the disturbance provided by the input signal is attenuated along the string (the respective signal amplitudes decrease along the string). This confirms strict string stability. Furthermore, the experiments show that the design

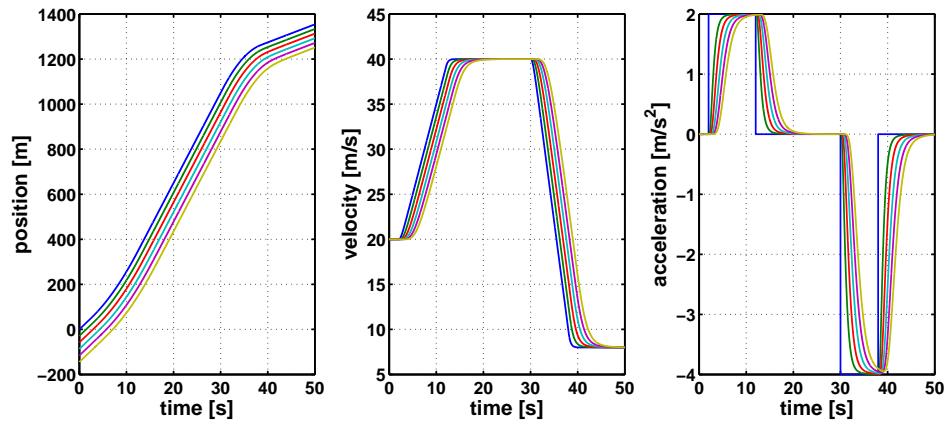


Figure 25: CACC design for 0.1s delay by second-order Padé-approximation.

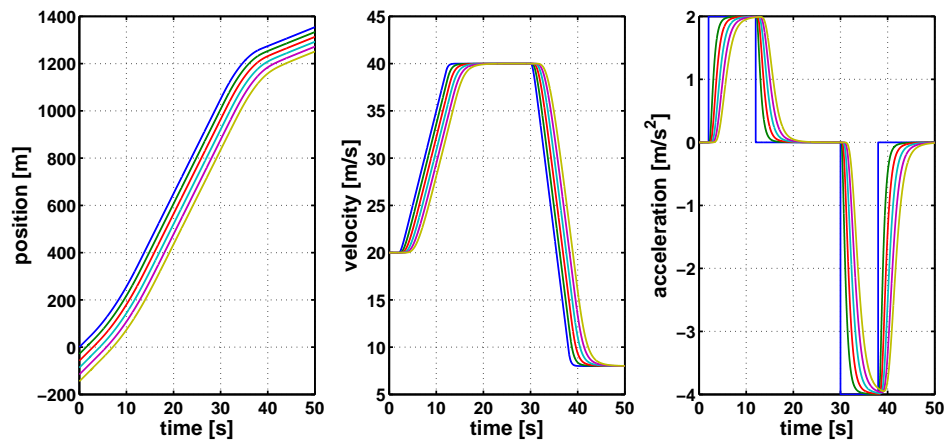


Figure 26: CACC design for 0.1s delay by fifth-order Padé-approximation.

by different orders of Padé-approximation lead to similar results for string stability and fast following vehicles.

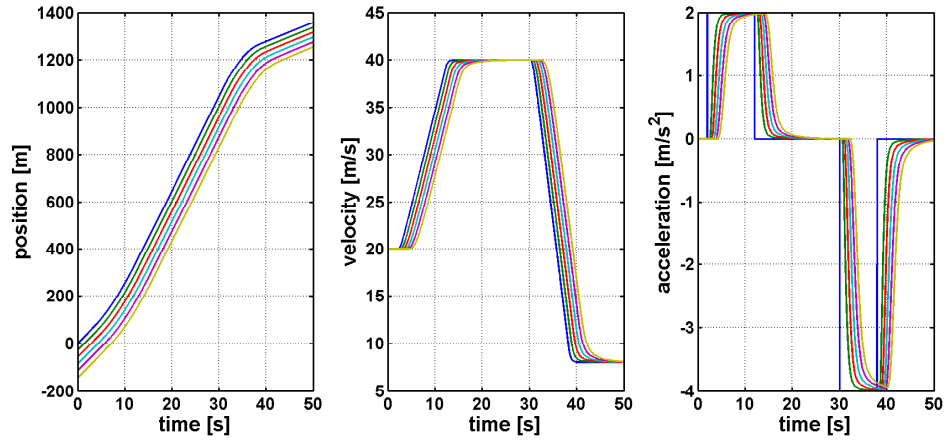


Figure 27: CACC design for 0.3s delay by second-order Padé-approximation.

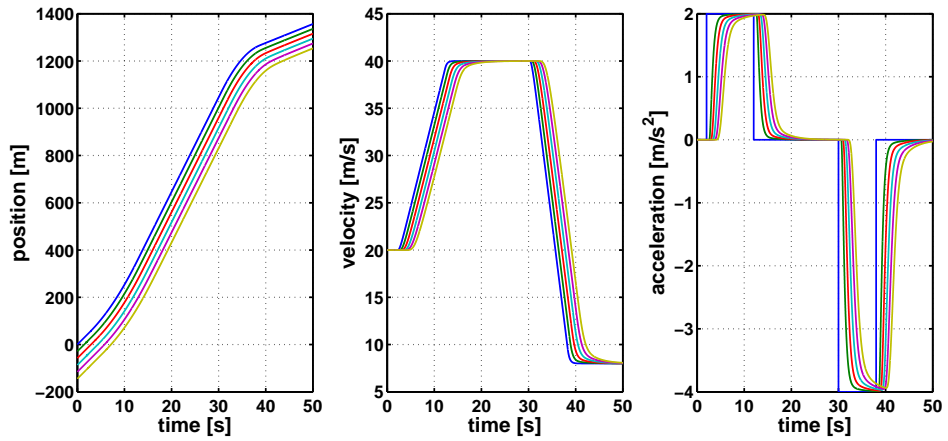


Figure 28: CACC design for 0.3s delay by fifth-order Padé-approximation.

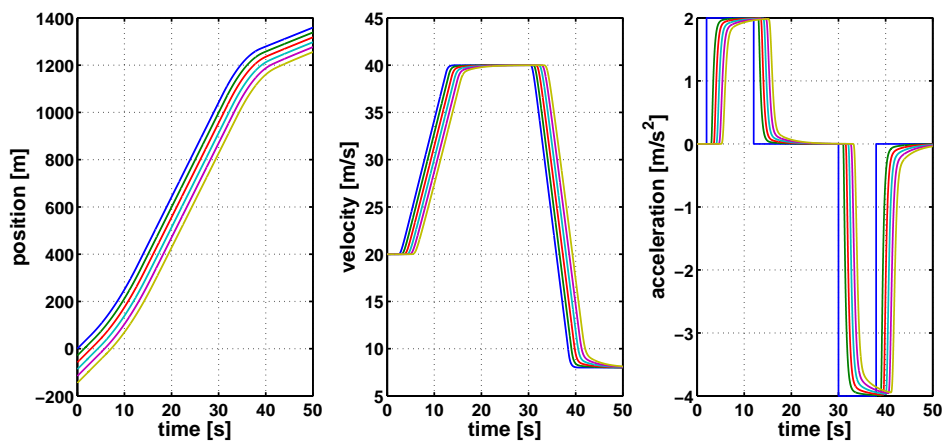


Figure 29: CACC design for 0.5s delay by second-order Padé-approximation.

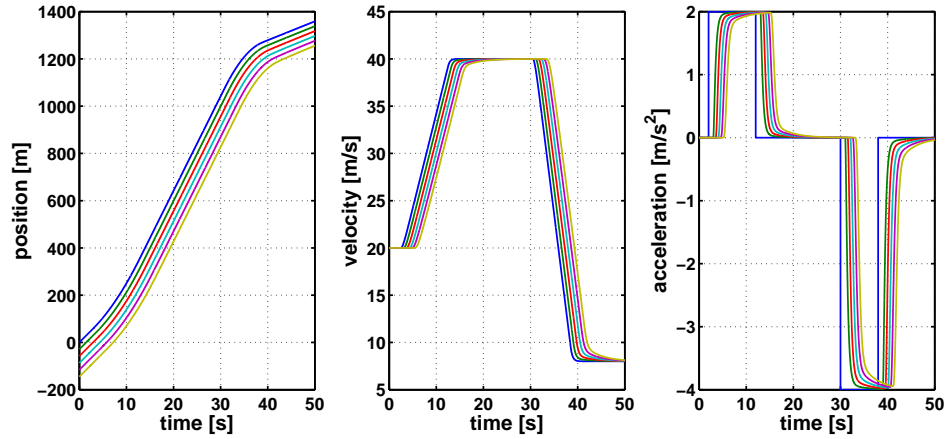


Figure 30: CACC design for 0.5s delay by fifth-order Padé-approximation.

4.5 Smith-Predictor

The Smith predictor has an important role in the control of time-delay systems which is efficient for processes with long time-delay [28]. It was discovered in 1957 by Otto J. M. Smith. Smith-predictor design is based on an inner loop with a main controller that can simply be designed without the time-delay. The result is that the delay is shifted outside the feedback loop [45, 46, 47]. The basic structure of the Smith-predictor is shown in Figure 31.

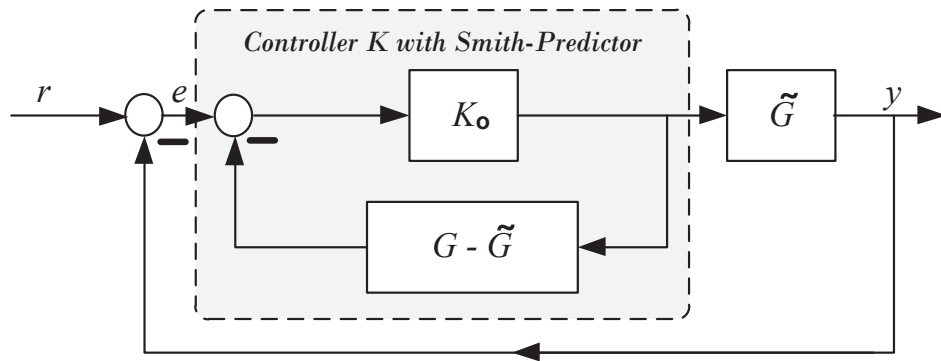


Figure 31: System with Smith-predictor loop.

$\tilde{G}(s) = e^{-sT} G(s)$ is a plant system with a delay, where the Smith predictor is represented as $SP = G(s) - e^{-sT} G(s)$. $G(s)$ is the rational part of $\tilde{G}(s)$ (without delay) [28, 44, 53]. It can be seen that the delay is moved outside the feedback loop and the

main controller $K(s)$ can be designed according to the delay-free part $G(s)$ of only the plant as seen in (4.13).

$$K(s) = \frac{K_o(s)}{1 + K_o(s)(G(s) - e^{-sT}G(s))}. \quad (4.13)$$

4.5.1 Modified CACC with Smith-Predictor

We add the Smith-predictor to the feedback loop. The new modification of CACC with Smith-predictor is shown in Figure 32. Here, $G(s)$ is a rational dynamic vehicle

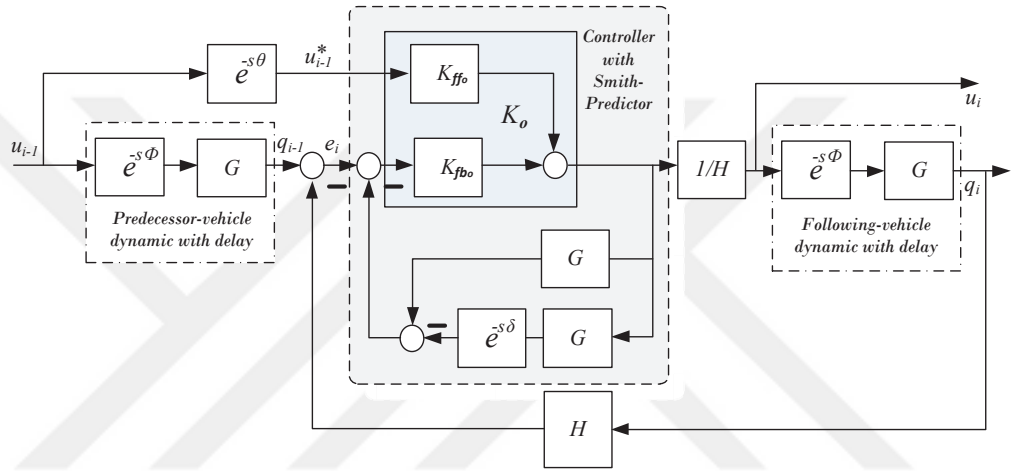


Figure 32: CACC model with smith-predictor.

(without delay), θ refers to communication delay, ϕ represents internal dynamic delay and δ is assumed as a mutual delay between communication delay and internal dynamic delay. The main controller $K_o(s)$ is represented as:

$$K_o(s) = \begin{bmatrix} K_{ffo} & K_{fbo} \end{bmatrix}. \quad (4.14)$$

To this end, the controller $K(s)$ is computed as the main controller with Smith-predictor loop.

$$K(s) = \begin{bmatrix} K_{ffo} & \frac{K_{fbo}(s)}{1 + K_{fbo}(s)(G(s) - e^{-sT}G(s))} \end{bmatrix}. \quad (4.15)$$

4.5.2 Modified CACC with Smith-Predictor for $\theta=\phi$ Case

In the case $\theta=\phi$, the H_∞ control computation can be easily performed, because the CACC loop with Smith-predictor does not include any delay. That is, all delays are moved out of the feedback loop. The new block diagram is displayed in Figure 33. The δ value is assumed to be the same as θ, ϕ value. Again, the H_∞ control for a

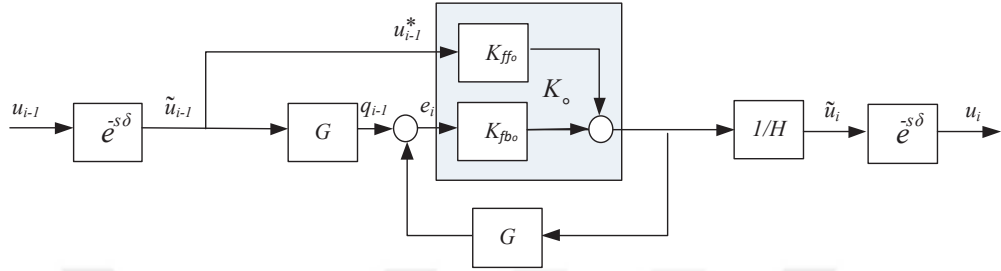


Figure 33: Modified CACC in $\theta=\phi$ case .

CACC model with Smith-predictor is formulated to minimize the position error $e_i(t)$ and achieve string-stability (4.11). That is, we want

$$\min_K \left\| \begin{array}{c} \Gamma(s) \\ S(s) \end{array} \right\|_\infty \leq 1 \quad (4.16)$$

where $\Gamma(s)$ is given as:

$$\Gamma(s) := \Gamma_i(s) = \frac{\tilde{U}_i(s)}{\tilde{U}_{i-1}(s)} = \frac{K_{ffo} + G_i K_{fbo}}{H(1 + G_i K_{fbo})}. \quad (4.17)$$

and $S(s)$ is a sensitivity:

$$S(s) = \frac{E_i(s)}{\tilde{U}_{i-1}(s)} = \frac{G(1 - K_{ffo})}{1 + G K_{fbo}}. \quad (4.18)$$

For this purpose, the lower fractional transformation (LFT) and the corresponding matrix P are as shown in Figure 34.

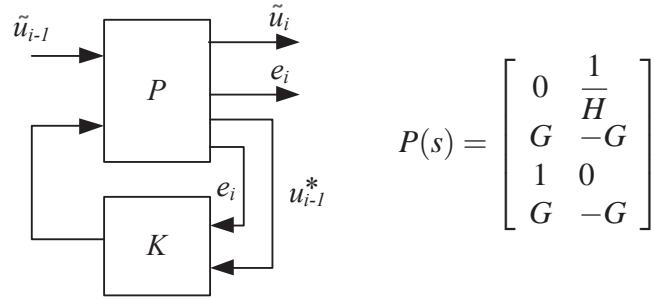


Figure 34: Structure of H_∞ control for CACC with Smith-predictor.

4.5.3 Experimental Results

The simulations are performed to confirm a vehicle platoon with string-stability for the modified CACC with Smith-predictor for different delay scenarios. These simulations are executed with the same parameters and input that are used in Section 4.4.2. It can be seen that string-stability is indeed achieved in all cases.

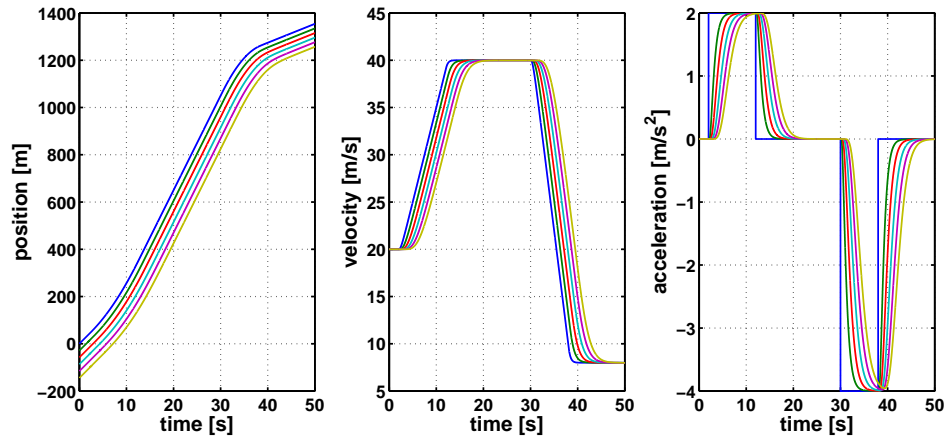


Figure 35: CACC with Smith-predictor design for string stability with 0.1s delay.

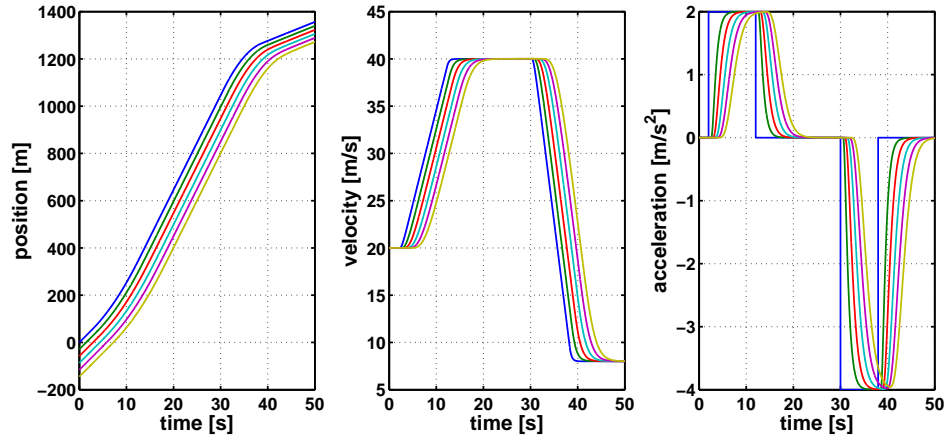


Figure 36: CACC with Smith-predictor design for string stability with 0.3s delay.

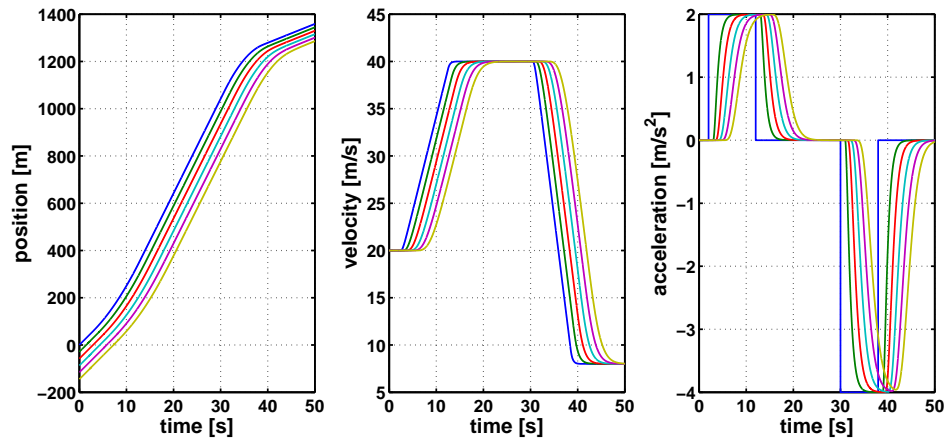


Figure 37: CACC with Smith-predictor design for string stability with 0.5s delay.

4.6 Finite Impulse Response (FIR) Blocks

Finite impulse response (FIR) blocks are frequently used as solution for control of time-delay systems. The FIR operator divides into the completion operator and the truncation operator [28]. Consider

$$G(s) = \left[\begin{array}{c|c} A & B \\ \hline C & D \end{array} \right] \quad (4.19)$$

is a rational transfer matrix (without delay) such that $G(s) = C(sI - A)^{-1}B$. To this end, the following two operators combined with $G(s)$ are widely used as:

the *truncation operator* $\tau_T\{G\}$ is defined as:

$$\begin{aligned}\tau_T\{G\} &= \left[\begin{array}{c|c} A & B \\ \hline C & D \end{array} \right] - e^{-sT} \left[\begin{array}{c|c} A & e^{AT}B \\ \hline C & 0 \end{array} \right] \\ &= C(I - e^{(-sI-A)T})(sI - A)^{-1}B = G - e^{-sT}\tilde{G}\end{aligned}\quad (4.20)$$

and the *completion operator* $\pi_T\{e^{-sT}G\}$ is defined as:

$$\begin{aligned}\pi_T\{e^{-sT}G\} &= \left[\begin{array}{c|c} A & B \\ \hline Ce^{-AT} & 0 \end{array} \right] - e^{-sT} \left[\begin{array}{c|c} A & B \\ \hline C & D \end{array} \right] \\ &= Ce^{-sT}(I - e^{(-sI-A)T})(sI - A)^{-1}B = \hat{G} - e^{-sT}G\end{aligned}\quad (4.21)$$

These two operators map any rational transfer matrix into an FIR block. It can be verified that both $\pi_T\{e^{-sT}G\}$ and $\tau_T\{G\}$ are entire functions whose impulse responses have finite support (FIR systems) [28, 54, 55].

4.6.1 Modified CACC By FIR Block In Same Delays Case

In order to extend CACC by an FIR block, firstly CACC is modified in a way that all delays move out of the closed loop as shown in Figure 38. Then, assume that the

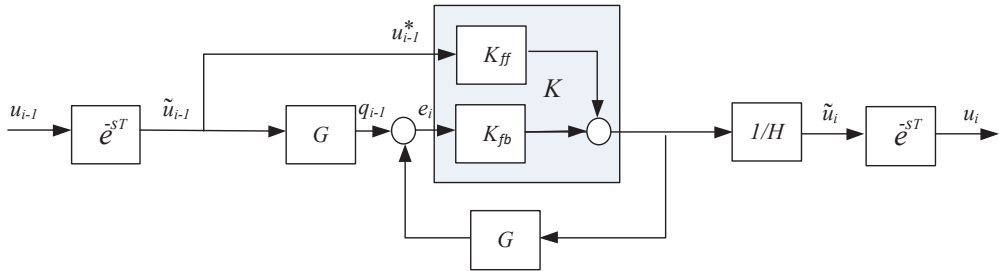


Figure 38: Modified CACC model in same delays case.

$\pi_T\{e^{-sT}G\}$ operator is appropriate for CACC model. The new extension of CACC model is by inserting FIR block to the feedback loop as shown in Figure 39.

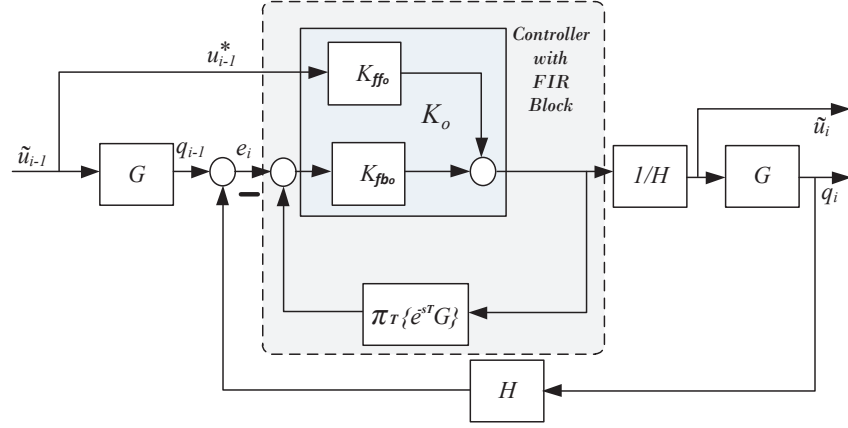


Figure 39: CACC with FIR block.

Here,

$$\hat{G}(s) = \left[\begin{array}{c|c} A & B \\ \hline C e^{-AT} & 0 \end{array} \right] \quad (4.22)$$

is a plant including the value of the delay, which is represented as T . After modification as seen in Figure 40, it can be concluded that the FIR block removes all delays from system. The controller $K(s)$ can be designed according to the main controller with FIR block as seen in (4.23).

$$K(s) = \left[K_{ffo} \frac{K_{fbo}}{1 + K_{fbo} \hat{G}} \right] \quad (4.23)$$

4.6.2 String Stability

We want that the transfer function $\Gamma(s)$ from $U_i(s)$ to $U_{i-1}(s)$ fulfills the string stability condition of a platoon of vehicles;

$$\Gamma(s) := \Gamma_i(s) = \frac{U_i(s)}{U_{i-1}(s)} = \frac{e^{-s\theta_i} K_{ffo} + e^{-s\phi_i} G_i K_{fb}}{H (1 + e^{-s\phi_i} G_i K_{fb})}, \quad (4.24)$$

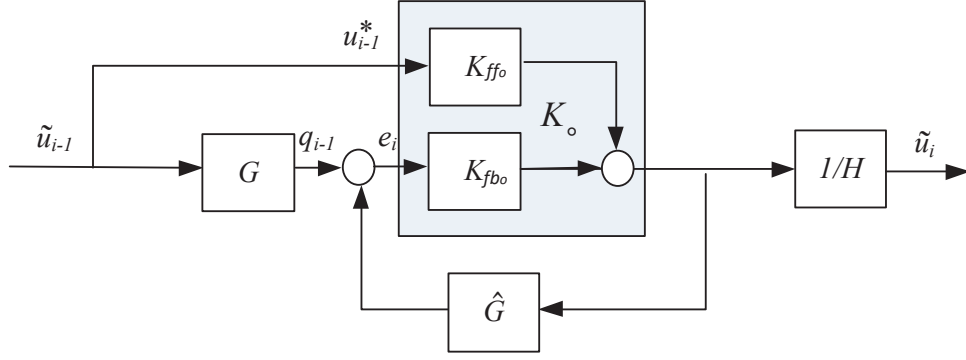


Figure 40: Modified CACC by using FIR block.

where the feedback controller K_{fb} represents the main controller K_{fb0} with FIR block as shown in (4.25);

$$K_{fb}(s) = \frac{K_{fb0}}{1 + K_{fb0}FIR}. \quad (4.25)$$

To this end, the strict string stability is achieved if for all vehicles i

$$\|\Gamma_i(s)\|_\infty \leq 1. \quad (4.26)$$

4.6.3 H_∞ control Structure

In order to design H_∞ control such that string stability is fulfilled (4.26) and at the same time we minimize the position error $e_i(t)$, the H_∞ control problem is written as

$$\min_K \left\| \begin{array}{c} \Gamma(s) \\ S(s) \end{array} \right\|_\infty \leq 1 \quad (4.27)$$

where, Γ is obtained from Figure 40 as:

$$\Gamma(s) := \Gamma_i(s) = \frac{\tilde{U}_i(s)}{\tilde{U}_{i-1}(s)} = \frac{K_{ff0} + G_i K_{fb0}}{H(1 + \hat{G}_i K_{fb0})}. \quad (4.28)$$

$S(s)$ is the closed-loop sensitivity corresponding to vehicle i as shown in (4.29).

$$S(s) = \frac{E_i(s)}{\tilde{U}_{i-1}(s)} = \frac{G_i + \hat{G}_i K_{ff0}}{1 + G_i K_{fb0}}. \quad (4.29)$$

This method is proposed for designing the main controller K_o under the requirements of string stability, which can be written as:

$$K_o = \begin{bmatrix} K_{ffo} & K_{fbo} \end{bmatrix}. \quad (4.30)$$

To this end, the lower fractional transformation (LFT) with the corresponding matrix P are shown in Figure 41 as evaluated from Figure 40.

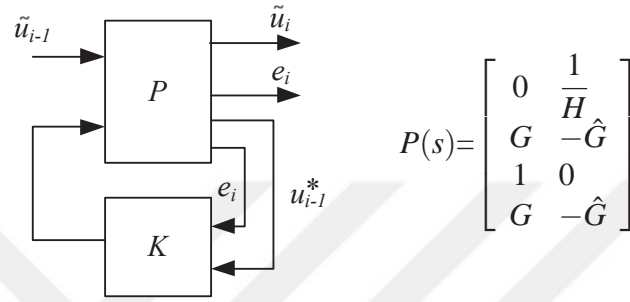


Figure 41: H_∞ design for CACC with FIR block.

4.6.4 Simulation Results

For simulations of CACC with FIR block model, it performs the same parameters and input as in Section 4.4.2. In addition, T is considered same as ϕ .

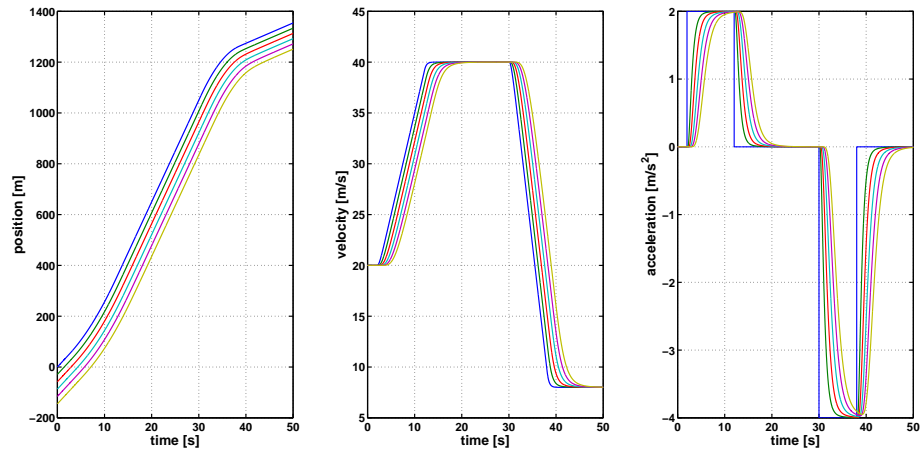


Figure 42: CACC with FIR block for string stability with 0.1s delay.

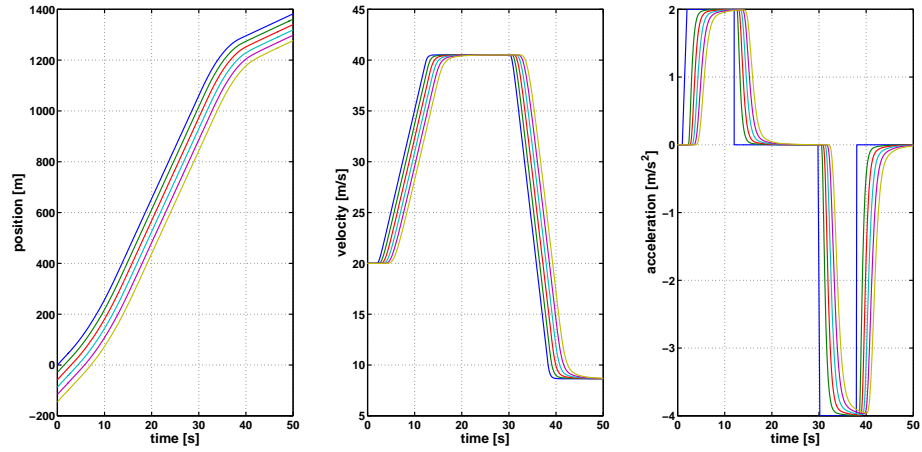


Figure 43: CACC with FIR block For string stability with 0.3s delay.

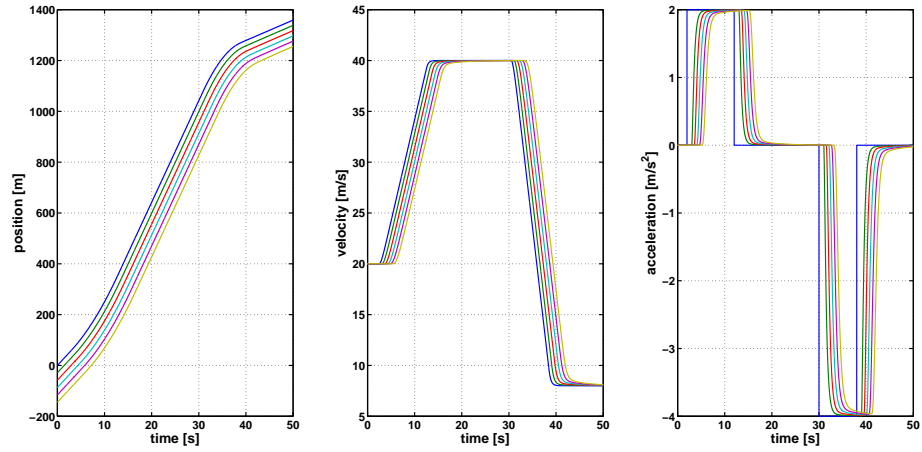


Figure 44: CACC with FIR block for string stability with 0.5s delay.

4.7 A Transformed Standard H_∞ Problem

4.7.1 Introduction

A transformed standard H_∞ Problem is used to solve the H_∞ control of time-delay systems by Qing-Chang Zhong [28]. This method is based on a transformed delay in the H_∞ design which is presented as a beneficial way to compute the H_∞ norm with delay. With this transformation, all robust control problems can be solved analogous to the finite-dimensional versions. In addition, this transformation has a trade-off in the performance such that the controller obtained has a quite simple and transparent structure with a modified Smith-predictor. Moreover, there are no additional hidden modes in the Smith predictor. To this end, the practical significance of the approach is

obvious.

Let,

$$G(s) = \left[\begin{array}{c|c} A & B \\ \hline C & D \end{array} \right] \quad (4.31)$$

with the rational plant transfer function $G(s) = C(sI - A)^{-1}B$. The transformation uses truncation operator $\tau_T\{G\}$ and completion operator $\pi_T\{e^{-sT}G\}$ as defined in Section 4.6, such that these two operators map any rational transfer matrix into an FIR block.

4.7.2 Transformation

Consider the standard feedback configuration with delay shown in Figure 45. It consists of the interconnected plant P and a general controller $K(s)$ with delay.

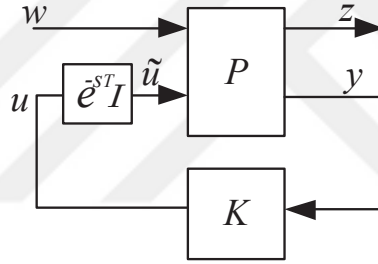


Figure 45: General control setup for time-delay systems.

Consider P as

$$P(s) = \begin{bmatrix} P_{11} & P_{12} \\ P_{21} & P_{22} \end{bmatrix} \quad (4.32)$$

The closed-loop transfer matrix from w to z is:

$$TF_{zw}(s) = P_{11} + e^{-sT}P_{12}K(I - e^{-sT}P_{22}K)^{-1}P_{21}. \quad (4.33)$$

Then, the FIR block is represented as

$$\Delta_1(s) = \tau_T\{P_{11}\} = P_{11} - \tilde{P}_{11}(s)e^{-sT}. \quad (4.34)$$

Subtracting it from the feed-forward path P_{11} , as shown in Figure 47, we obtain

$$TF_{zw}(s) = \Delta_1(s) + T_{z'w}(s). \quad (4.35)$$

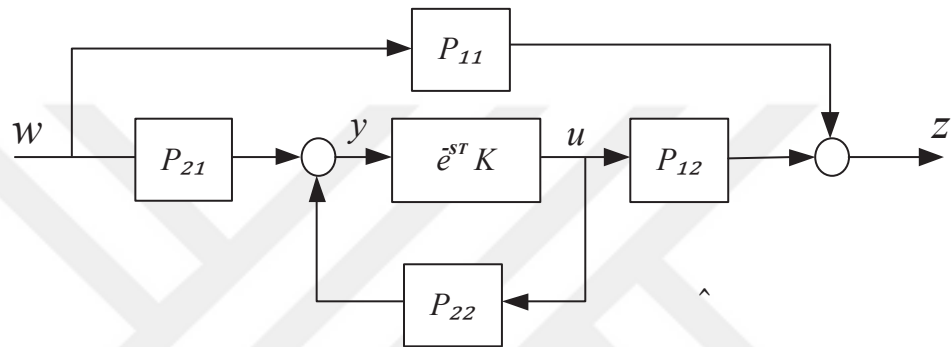


Figure 46: An equivalent structure.

That is,

$$TF_{z'w}(s) = e^{-sT} \{ \tilde{P}_{11} + P_{12}K(I - e^{-sT}P_{22}K)^{-1}P_{21} \}. \quad (4.36)$$

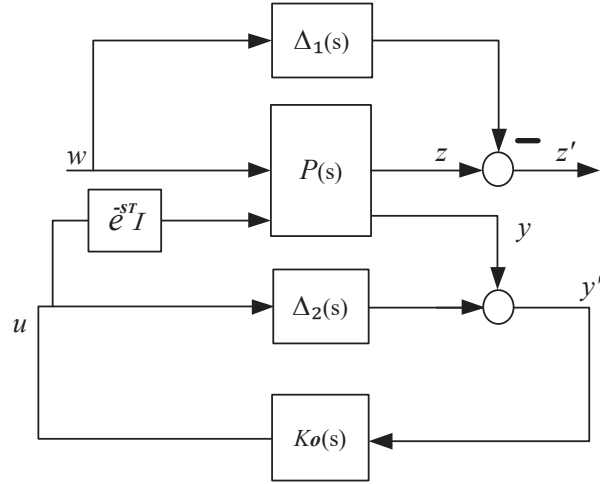


Figure 47: The graphic interpretation of the transformation.

4.7.3 H_∞ Control Design with a Single Delay

Assume that the realization of the rational part of the generalized process in Figure 45 is taken to be of the form

$$P(s) = \left[\begin{array}{c|cc} A & B_1 & B_2 \\ \hline C_1 & D_{11} & D_{12} \\ C_2 & D_{21} & D_{22} \end{array} \right] \quad (4.37)$$

then, we suppose that the system parameter matrices satisfy the following assumptions:

A1) (A, B_2) is stabilizable and (C_2, A) is detectable;

A2) $\begin{bmatrix} A - j\omega I & B_2 \\ C_1 & D_{12} \end{bmatrix}$ has full column rank $\forall \omega \in R$;

A3) $\begin{bmatrix} A - j\omega I & B_1 \\ C_2 & D_{21} \end{bmatrix}$ has full row rank $\forall \omega \in R$;

A4) $D_{12}^* D_{12} = I$ and $D_{21} D_{21}^* = I$.

Assumption (A4) is made to simplify the exposition. Factually, only the non-singularity of the matrices $D_{12}^* D_{12}$ and $D_{21} D_{21}^*$ is required.

Now consider a Smith predictor-type controller:

$$K(s) = K_o(s)(I - \Delta_2(s)K_o(s))^{-1} \quad (4.38)$$

as shown in figure 47. The predictor is designed to be

$$\Delta_2(s) = \pi_T \{ e^{-sT} P_{22} \} = \left[\begin{array}{c|c} A & B_2 \\ \hline C_2 e^{-AT} & 0 \end{array} \right] - e^{-sT} \left[\begin{array}{c|c} A & B_2 \\ \hline C_2 & D_{22} \end{array} \right] \quad (4.39)$$

then, the system can be re-formulated as

$$\begin{bmatrix} z'' \\ y' \end{bmatrix} = \tilde{P}(s) \begin{bmatrix} w \\ u \end{bmatrix}, \quad (4.40)$$

$$u = k_o(s)y' \quad (4.41)$$

with $e^{-sT} z'' = z'$, where

$$\tilde{P}(s) = \left[\begin{array}{cc|cc} A & & e^{AT} B_1 & B_2 \\ \hline C_1 & & 0 & D_{12} \\ C_2 e^{-AT} & & D_{21} & 0 \end{array} \right]. \quad (4.42)$$

The closed-loop transfer function from w to z' becomes

$$TF_{z'w}(s) = e^{-sT} TF_{z''w}(s) = e^{-sT} \mathcal{F}_l(\tilde{P}(s), K_o(s)). \quad (4.43)$$

Hence, the H_∞ control problem

$$\|TF_{z'w}(s)\|_\infty < \gamma. \quad (4.44)$$

is converted to

$$\|\mathcal{F}_l(\tilde{P}(s), K_o(s))\|_\infty < \gamma. \quad (4.45)$$

The solution of the H_∞ control involves two Hamiltonian matrices;

$$H_T = \begin{bmatrix} A & \gamma^{-2}e^{AT}B_1B_1^*e^{A^*T} \\ -C_1^*C_1 & -A^* \end{bmatrix} - \begin{bmatrix} B_2 \\ -C_1^*D_{12} \end{bmatrix} \begin{bmatrix} D_{12}^*C_1 & B_2^* \end{bmatrix}, \quad (4.46)$$

and

$$J_T = \begin{bmatrix} A^* & \gamma^{-2}C_1^*C_1 \\ -e^{AT}B_1B_1^*e^{A^*T} & -A \end{bmatrix} - \begin{bmatrix} e^{-A^*T}C_2^* \\ -e^{AT}B_1D_{21}^* \end{bmatrix} \begin{bmatrix} D_{21}B_1^*e^{A^*T} & C_2e^{-AT} \end{bmatrix}. \quad (4.47)$$

Theorem 2. *There exists an admissible main controller such that $\|T_{z'w}(s)\|_\infty < \gamma$, if and only if the following three conditions hold:*

- (i) $H_T \in \text{dom}(\text{Ric})$ and $X = \text{Ric}(H_T) \geq 0$;
- (ii) $J_T \in \text{dom}(\text{Ric})$ and $Y = \text{Ric}(J_T) \geq 0$;
- (iii) $\rho(XY) < \gamma^2$.

Moreover, when the conditions hold, one such main controller is:

$$K_o(s) = \left[\begin{array}{c|c} A_T & -L_T \\ \hline F_T Z_T & 0, \end{array} \right] \quad (4.48)$$

where

$$A_T = A + L_T C_2 e^{-AT} + \gamma^{-2} Y C_1^* C_1 + (B_2 + \gamma^{-2} Y C_1^* D_{12}) F_T Z_T, \quad (4.49)$$

$$F_T = -(B_2^* X + D_{12}^* C_1). \quad (4.50)$$

$$L_T = -(Y e^{-A^*T} C_2^* + e^{AT} B_1 D_{21}^*). \quad (4.51)$$

$$Z_T = (I - \gamma^{-2} Y X)^{-1}. \quad (4.52)$$

Furthermore, the set of all admissible main controllers such that $\|T_{z'w}(s)\|_\infty < \gamma$ can be parameterized as

$$K_o(s) = \mathcal{F}_l(M(s), Q(s)) \quad (4.53)$$

where

$$M(s) = \left[\begin{array}{c|cc} A_T & -L_T & B_2 + \gamma^{-2} Y C_1^* D_{12} \\ \hline F_T Z_T & 0 & I \\ -(C_2 e^{-AT} + \gamma^{-2} D_{21} B_1^* e^{A^* T} X) Z_T & I & 0 \end{array} \right] \quad (4.54)$$

and $Q(s) \in H_\infty$, $\|Q(s)\|_\infty < \gamma$.

4.7.4 CACC Design by A Transformed Standard H_∞ Problem

Consider our CACC model as shown in Figure 20 is designed by H_∞ control with

$$\min_K \left\| \begin{bmatrix} \Gamma(s) \\ S(s) \end{bmatrix} \right\|_\infty \leq 1, \quad (4.55)$$

where $\Gamma(s)$ and $S(s)$ are as seen in (4.3), (4.6) respectively. Then, the lower fractional transformation (LFT) with the corresponding matrix P are as shown in Figure 48 as evaluated from Figure 20.

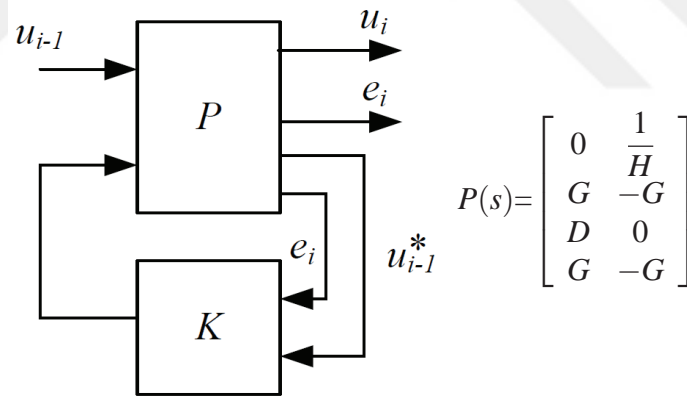


Figure 48: Structure of H_∞ optimal control for CACC model.

The new control design of CACC model by a transformed standard H_∞ problem is evaluated as shown in Figure 49. Here, $\Delta_1(s)$ is neglected due to $P_{11} = 0$ in CACC model, so it has no any affect on the string-stability if there is $\Delta_1(s)$ or not. $\Delta_2(s)$ is computed according to (4.39), then it is added to the closed-loop part in CACC model. In addition, the conditions of $D_{12}^* D_{12} = I$ and $D_{21} D_{21}^* = I$ are met by adding a new row $[0 \ 1]$ in the 3rd column of P for regularization (this means the extra output (E_o))

is assumed to be the same as the model given in Figure 49). To this end, the control design is formulated for:

$$\min_K \left\| \begin{array}{c} \Gamma(s) \\ S(s) \\ E_o(s) \end{array} \right\|_{\infty} \leq 1 \quad (4.56)$$

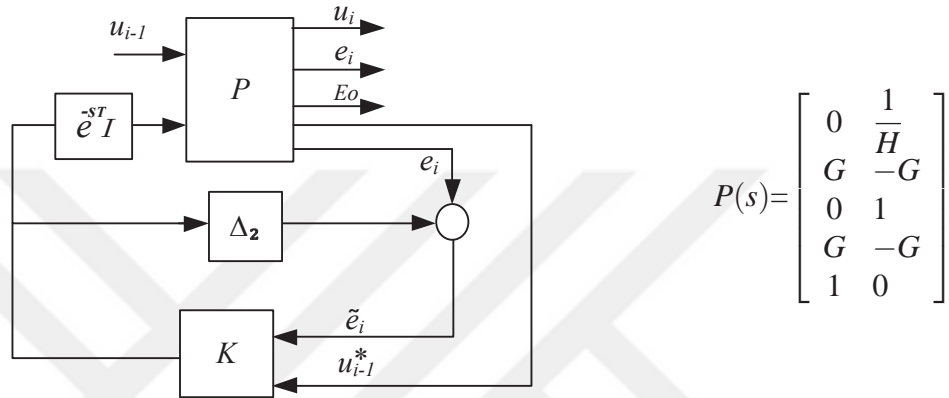


Figure 49: Structure of a transformed standard H_{∞} for CACC model.

4.7.5 Simulation Results

Consider a CACC model with delays using the transformed standard H_{∞} method. The simulations are performed with the same parameters and input used in Section 4.4.2. Figures 50, 50 and 50 show the impact of design by a transformed standard H_{∞} control on the string-stability.

4.8 Discussion

In this chapter we provide many methods to find a useful solution for CACC design with delay. Controller with predictor gives a good performance for obtaining string-stability. In the first method, the dynamic and communication delay are converted to the rational transfer function by using Padé-approximations with different orders. Whereas, in the design by Smith-predictor or FIR blocks, it is assumed that predictor

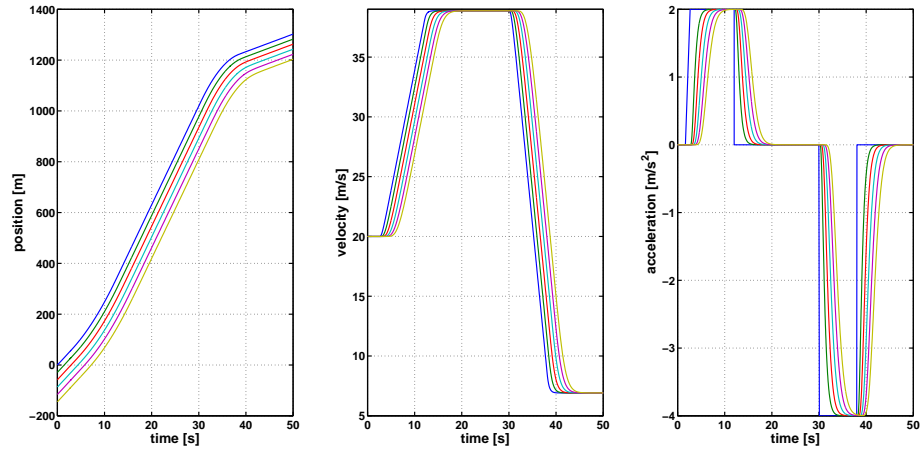


Figure 50: CACC design by a transformed standard H_∞ with 0.1s delay.

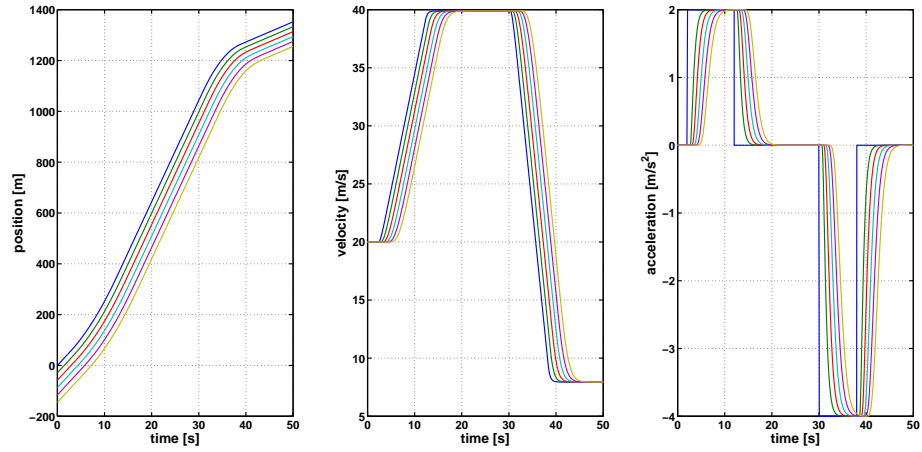


Figure 51: CACC design by a transformed standard H_∞ with 0.3s delay.

helps moving all delays out of the closed-loop. For this reason H_∞ control design is easy to compute. However, in the last method, the solvability conditions of the standard H_∞ problem with a delay depends on a transformed delay in the H_∞ design. The existence of solutions then depends on two delay-independent algebraic Riccati equations and the non-singularity property of a delay-dependent matrix.

4.8.1 Simulation Results for Comparison

In comparison experiments, we execute each simulation with a string of 2 vehicles, considering the same parameters and input as in Section 4.4.2. Figures 53, 54 and 55 show that the controller design by using Padé-approximation and FIR blocks lead to a faster response than the design by Smith-predictor or transformed standard H_∞ control.

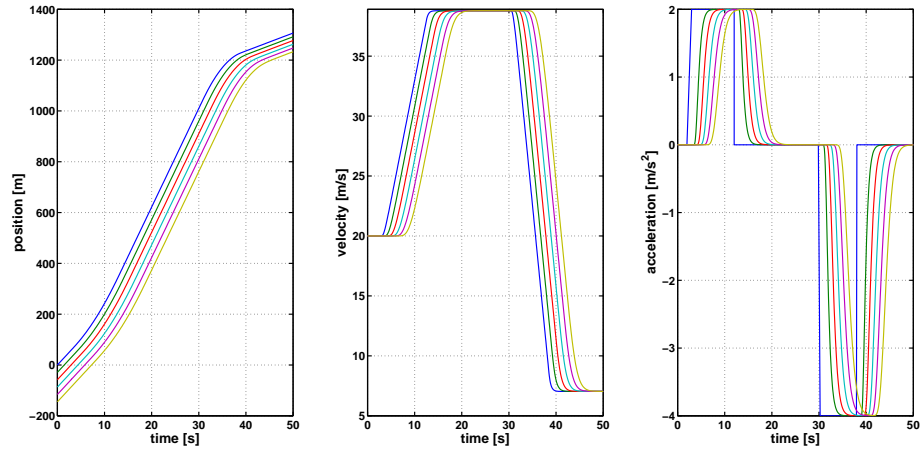


Figure 52: CACC design by a transformed standard H_∞ with 0.5s delay.

This is true for both small and large delays. Furthermore, we support the figures by zooming in order to show the vehicle motion for each method.

4.8.2 Headway Time Problem

The main objective of CACC in vehicle platoon is to design controllers that obtain a safe and stable vehicle following at small inter-vehicle spacing by a small headway time. In order to check the headway for each method, we perform some simulations with different scenarios of delays. We consider same input and parameters as used in Section 4.4.2 . The experiments show that the controller design for very small delays by using Padé-approximation or FIR block gives string-stability for a very small headway. However, the disadvantage of these two methods is seen when the delay increases. Then, the headway needs to be large in order to achieve string-stability. In addition, it has to be noted that the controller order can be very high when using the Padé-approximation (see Table 10). Whereas, the Smith predictor works for all values of delays (large or small) but can not support very small headway times. Finally, the transformed standard H_∞ method works for large headway times. The computation for small headway times causes numerical problems in the solution of the Riccati equations. The tables below show the results for different delays and methods.

<i>Method</i>	<i>String-stability if headway \leq</i>
Padé-approximation	0.101
FIR block	0.11
Smith predictor	0.301
A Transformed Standard H_∞	0.5

Table 4: Control design for 0.1 delay.

<i>Method</i>	<i>String-stability if headway \leq</i>
Padé-approximation	0.32
FIR block	0.31
Smith predictor	0.301
A Transformed Standard H_∞	0.5

Table 5: Control design for 0.3 delay.

<i>Method</i>	<i>String-stability if headway \leq</i>
Padé-approximation	0.56
FIR block	0.53
Smith predictor	0.301
A Transformed Standard H_∞	0.5

Table 6: Control design for 0.5 delay.

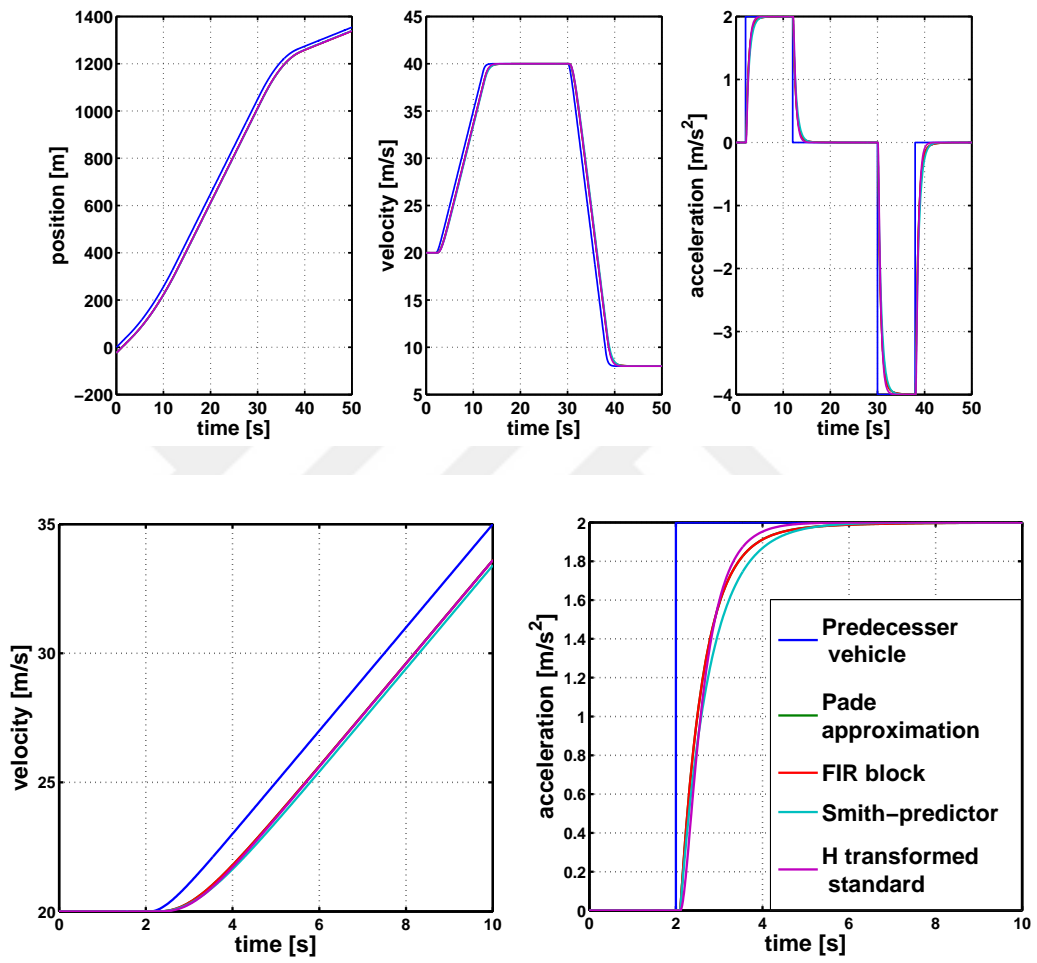


Figure 53: Design methods for string stability with 0.1s delay.

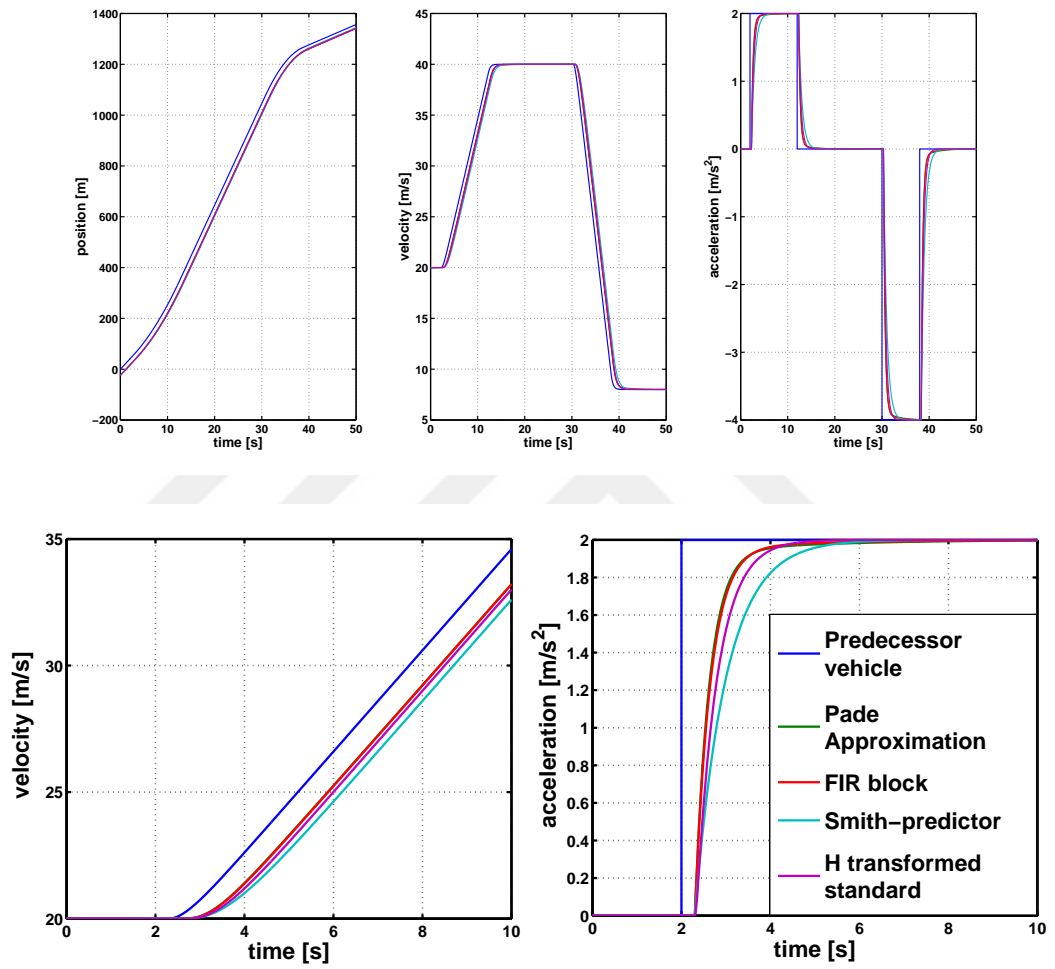


Figure 54: Design methods for string stability with 0.3s delay.

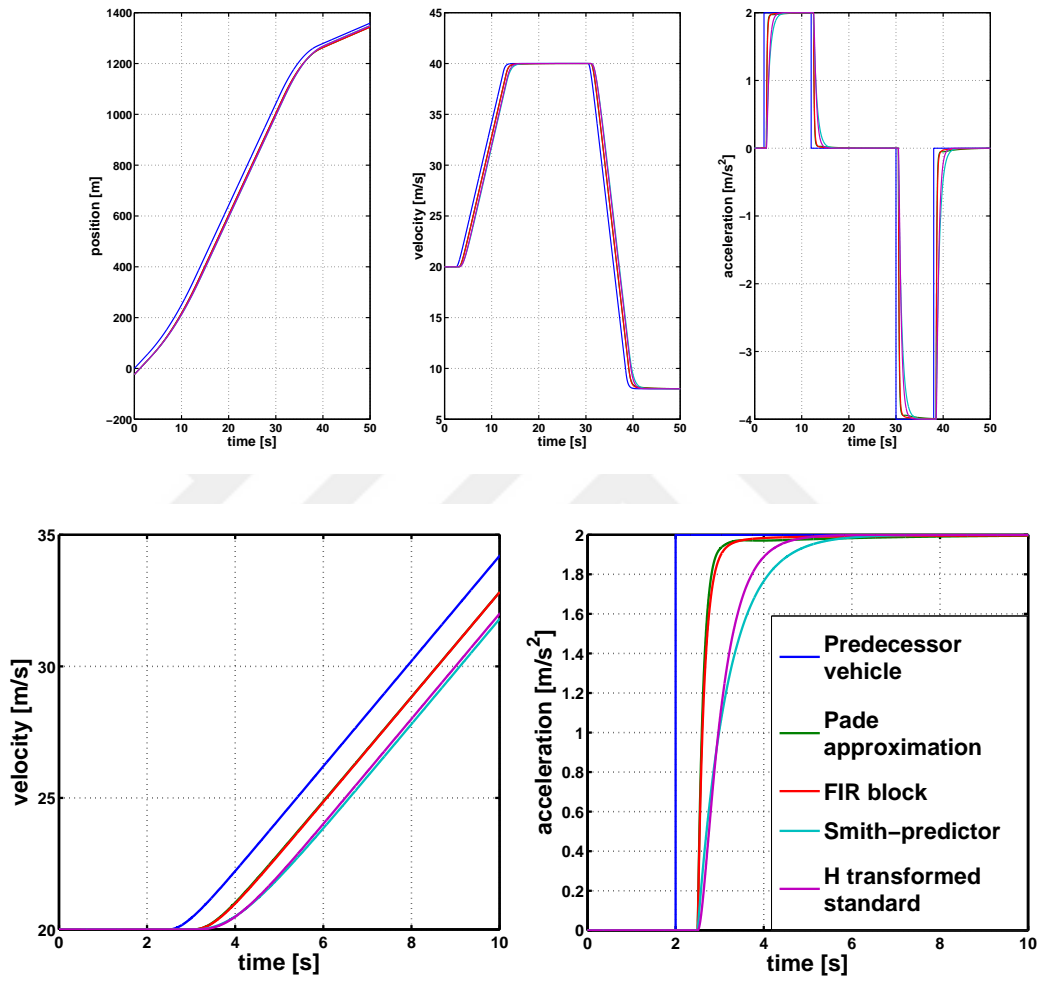


Figure 55: Design methods for string stability with 0.5s delay.

CHAPTER 5

CONCLUSION AND FUTURE WORK

This thesis developed H_∞ controller design methods for Cooperative Adaptive Cruise Control (CACC) in string of vehicles in platoon. Here, it is desired to realize a short distance between vehicles in order to increase the traffic throughput, whereas driving safety must be ensured.

The first part of this thesis presents the general background about CACC and vehicle motion with the definition of string-stability. Moreover, the H_∞ controller design for homogeneous vehicles is introduced. The second part of this thesis, develops a new H_∞ control method that ensures strict stability for heterogeneous vehicle strings. That is, velocity and acceleration disturbances in the string are attenuated along the string even if the string is composed of vehicles with different dynamic properties. String stability is analytically evaluated and also supported by results from simulation experiments. The third part of this thesis focuses on the design of CACC with delay by H_∞ control. In this thesis, different methods are suggested. In the first method, the communication and dynamic delays are converted to rational transfer function by using Padé-approximation. In the second and third methods, the CACC is modified by addition of a Smith-predictor or FIR block to the closed-loop section such that delays are shifted outside the feedback loop. In the last method, CACC is designed by a transformed standard H_∞ problem, which is based on a transformed delay. Simulation experiments are presented for each method and a comparison shows their advantages.

Some suggestions for future work, include the CACC design for heterogeneous vehicles include time-delays and the CACC design in the case that communication and dynamic delay are different.

REFERENCES

1. **Baskar L. D., De Schutter B., Hellendoorn J., Papp Z., (2011)**, “*Traffic Control and Intelligent Vehicle Highway; Systems: A Survey*”, IET Intell. Transp. Syst., Vol. 5, No. 1, pp. 38-52.
2. **Ioannou P. A. (ed), (1997)**, “*Automated Highway Systems*”, Springer-Verlag US.
3. **Chowdhury M. A., Sadek A. W., (2003)**, “*Fundamentals of Intelligent Transportation Systems Planning*”, Artech House, INC. pp. 1-7/35-55.
4. **Nasim R., Kasser A., (2012)**, “*Distributed Architectures for Intelligent Transport Systems: A Survey*”, IEEE Second Symposium on Network Cloud Computing and Application, pp. 130-136.
5. **Varaiya P., (1993)**, “*Smart Cars on Smart Roads: Problems of Control*”, Automatic Control, IEEE Transactions on, Vol.38, no.2, pp.195-207.
6. **Papageorgiou M., Diakaki C., Dinopoulou V., Kotsialos A., Wang Y., (2003)**, “*Review of Road Traffic Control Strategies*”, Proceedings of The IEEE, Vol. 91, No. 12, pp.2043-2067.
7. **Sussman, Joseph S., (2005)**, “*Perspectives on Intelligent Transportation Systems (ITS)*”, Springer US.
8. **Ghosh S., Lee. T. S., (2010)**, “*Intelligent Transportation Systems: Smart and Green Infrastructure Design*”, CRC press, Second Edition.
9. **Rafiq G., Talha B., Patzold M., Gato Luis J., Ripa G., Carreras I., Coviello C., Marzorati S., Perez Rodriguez G., Herrero G., Desaegeer M., (2013)**, “*What’s New in Intelligent Transportation Systems?: An Overview of European Projects and Initiatives*”, Vehicular Technology Magazine, IEEE , Vol. 8, No. 4, pp.45-69.

10. **Tang S., Li Z., Chen D., Chen Z., Liu W., Liu X., Li L., Shi X., (2014)**, “*Theme Classification and Analysis of Core Articles Published in IEEE Transactions on Intelligent Transportation Systems From 2010 to 2013*”, *Intelligent Transportation Systems, IEEE Transactions on*, Vol. 15, No. 6, pp. 2710-2719.
11. **Linder A., Kircher A., Vadeby A., Nygardhs S., (2007)**, “*Intelligent Transport Systems (ITS) in Passenger Cars and Methods for Assessment of Traffic Safety Impact*”, VTI, Report 604A.
12. **Ran B., Peter J. Jin, Boyce D., Tony Z. Qiu, Cheng Y., (2012)**, “*Perspectives on Future Transportation Research: Impact of Intelligent Transportation System Technologies on Next-Generation Transportation Modeling*”, Taylor and Francis Group, LLC, Vol. 16, No. 4, pp. 226-242.
13. **Naus G. J. L., Vugts R. A., Ploeg J., Van de Molengraft M. J. G., Steinbuch M., (2010)**, “*String-Stable CACC Design and Experimental Validation: A Frequency-Domain Approach*”, *IEEE Transactions on Vehicular Technology*, Vol. 59, No. 9, pp. 4268-4279.
14. **Fernandes P., Nunes U., (2012)**, “*Platooning With IVC-Enabled Autonomous Vehicles: Strategies to Mitigate Communication Delays, Improve Safety and Traffic Flow*”, *Intelligent Transportation Systems, IEEE Transactions on*, Vol. 13, No. 1, pp. 91-106.
15. **Ploeg J., Shukla D. P., Van De Wouw N., Nijmeijer H., (2014)**, “*Controller Synthesis for String Stability of Vehicle Platoons*”, *IEEE Transactions on Intelligent Transportation Systems*, Vol. 15, No. 2, pp. 854-865.
16. **Oncu S., Ploeg J., Van De Wouw N., Nijmeijer H., (2014)**, “*Cooperative Adaptive Cruise Control: Network-Aware Analysis of String Stability*”, *Intelligent Transportation Systems, IEEE Transactions On* , Vol. 15, No. 4, pp. 1527-1537.

17. **Kianfar R., Ali M., Falcone P., Fredriksson J., (2014)**, “*Combined Longitudinal and Lateral Control Design for String Stable Vehicle Platooning Within a Designated Lane*”, Intelligent Transportation Systems (ITSC), IEEE 17th International Conference on, IAN.14773285, pp. 1003-1008.
18. **Marsden G., McDonald M., Brackstone M., (2001)**, “*Towards an Understanding of Adaptive Cruise Control*”, Transportation Research Part C 9, pp. 33-51.
19. **Vahidi A., Eskandarian A., (2003)**, “*Research Advances in Intelligent Collision Avoidance and Adaptive Cruise Control*”, Intelligent Transportation Systems, IEEE Transactions on , Vol. 4, No. 3, pp. 143-153.
20. **Kesting A., Treiber M., Schnhof M., Helbing D., (2008)**, “*Adaptive Cruise Control Design for Active Congestion Avoidance*”, Transportation Research Part C 16, pp. 668-683.
21. **Milanés V., Shladover S. E., (2014)**, “*Modeling Cooperative and Autonomous Adaptive Cruise Control Dynamic Responses Using Experimental Data*”, Transportation Research Part C 48, pp. 285-300.
22. **Kerner, B. S., (2009)**, “*Introduction to Modern Traffic Flow Theory and Control: The Long Road to Three-Phase Traffic Theory*”, Springer, Berlin, New York.
23. **Ploeg J., Van De Wouw N., Nijmeijer H., (2014)**, “*Lp String Stability of Cascaded Systems: Application to Vehicle Platooning*”, Control Systems Technology, IEEE Transactions on, Vol. 22, No. 2, pp. 786-793.
24. **Dunbar W. B., Caveney D. S., (2012)**, “*Distributed Receding Horizon Control of Vehicle Platoons: Stability and String Stability*”, Automatic Control, IEEE Transactions on, Vol. 57, No. 3, pp. 620-633.

25. **Samad Kamal M. A., Imura J. I., Hayakawa T., Ohata A., Aihara K., (2014),** “*Smart Driving of a Vehicle Using Model Predictive Control for Improving Traffic Flow*”, IEEE Transactions on Intelligent Transportation Systems, Vol. 15, No. 2, pp. 878-888.

26. **Rajamani R., (2011),** “*Vehicle Dynamics and Control*”, Springer, 2nd Edition, pp. 1-9, Chapter-5.

27. **Naus G., Vugts R., Ploeg J., Van de Molengraft R., Steinbuch M., (2010),** “*Cooperative Adaptive Cruise Control, Design and Experiments*”, American Control Conference (ACC), DOI: 10.1109, pp. 6145-6150.

28. **Zhong Q. C., (2006),** “*Robust Control of Time-Delay Systems*”, Springer, pp. 1-10/22-45/129-135.

29. **Lunge A. , Borkar P., (2015),** “*A Review on Improving Traffic Flow Using Cooperative Adaptive Cruise Control System*”, IEEE Sponsored 2nd International Conference on Electronics and Communication System, pp. 1474-1479.

30. **Nowakowski C., Shladover S. E., Cody D., Bu F., O’Connell J., Spring J., Dickey S., Nelson D., (2011),** “*Cooperative Adaptive Cruise Control: Testing Drivers Choices of Following Distances*”, California Path Research Report, UCB-ITS-PRR-2011-01.

31. **Swaroop D. V. A. H. G., (1997),** “*String Stability of Interconnected Systems: An Application to Platooning In Automated Highway Systems*”, California Partners for Advanced Transit and Highways (PATH).

32. **Zhou K., Doyle J. C., Glover K., (1996),** “*Robust and Optimal Control*”, Prentice Hall, Englewood CLI S, New Jersey 07632, pp. 441-468.

33. **Chang S., Gordon T. J., (2008),** “*A Flexible Hierarchical Model-Based Control Methodology for Vehicle Active Safety Systems*”, Vol. 46 Sup. 1, pp. 36-75.

34. **Sheikholeslamm S., Desoert C. A., (1990)**, “*Longitudinal Control of a Platoon of Vehicles*”, Berkeley, CA 94720.

35. **Sheikholeslam S., Desoer C. A., (1991)**, “*Longitudinal Control of a Platoon of Vehicles; III: Nonlinear Model*”, UCB, ITS, PRR-90-1.

36. **Sheikholeslam S., Desoer C. A., (1992)**, “*A System Level Study of the Longitudinal Control of a Platoon of Vehicles*”, Berkeley, CA 94720, 286, Vol. 114.

37. **Kianfar R., Augusto B., Ebadighajari A., Hakeem U., Nilsson J., Raza A., Tabar R. S., Irukulapati N. V., Englund C., Falcone P., Papanastasiou S., Svensson L., Wymeersch H., (2012)**, “*Design and Experimental Validation of a Cooperative Driving System in the Grand Cooperative Driving Challenge*”, IEEE Transactions on Intelligent Transportation Systems, Vol. 13, No. 3, pp. 994-1007.

38. **Moklegaard L., Druzhinina M., Stefanopoulou A. G., (2002)**, “*Longitudinal Control of Commercial Heavy Vehicles Equipped with Variable Compression Brake*”, California Path Research Report, UCB, ITS, PRR-2002-13, MI 48109-2121, ISSN 1055-1425.

39. **Van de Molengraft M. J. G., Ploeg J., Naus G. J. L., (2009)**, “*String-Stable CACC Design and Experimental Validation*”, R.P.A, Vugts, TU/E Master's Thesis, pp. 17.

40. **Mirzal A., (2012)**, “*Stability Analysis and Compensation of Time Delays in Analog Control Systems*”, International Journal of Control and Automation Vol. 5, No. 4.

41. **Carr S., O’Dwyer A., (1999)**, “*Robust Controller Design for Time Delay Systems Using H_∞ Techniques*”, Proceedings of the Irish Signals and Systems Conference, pp. 45-52.

42. **Liu X., Goldsmith A., Mahal S. S., Hedrick J. K., (2001)**, “*Effects of Communication Delay on String Stability in Vehicle Platoons*”, IEEE Intelligent Transportation System Conference (ITSC), Oakland, U.S.A, pp. 625-630.
43. **Haykin S., Van Veen B., (2007)**, “*Signals and Systems*”, 2nd ED.
44. **Levine W. S., (1999)**, “*Control System Fundamentals*”, CRC Press, 1st ED, Chapter-10.
45. **Bahill A. T., (1983)**, “*A Simple Adaptive Smith-Predictor for Controlling Time-Delay Systems*”, IEEE Control Systems Magazine Vol. 3, No. 2, pp. 16-22.
46. **Brown C., Coomhs D. J., (1991)**, “*Notes on Control with Delay*”, Technical Report 387, The University of Rochester, Computer Science Department Rochester, New York 14627.
47. **Wang Z. Q., Skogestad S., (1991)**, “ *μ Analysis and Synthesis of Time Delay Systems Using Smith Predictor*”, Decision and Control, Proceedings of the 30th IEEE Conference on, Vol. 3, pp. 3033-3034.
48. **Vajta M., (2000)**, “*Some Remarks on Padé-Approximations*”, 3rd Tempus-Intcom Symposium, September 9-14, Veszprém, Hungary.
49. **Gao D. Y., Krysko V. A., (2006)**, “*Introduction to Asymptotic Methods*”, Taylor and Francis Group, Chapman, Hall/CRC, Chapter-5.
50. **Gupta S. K., (1995)**, “*Numerical Methods for Engineers*”, ISBN: 81-224-0651-3, pp. 149-153.
51. **Wang Z., Hu. H., (1999)**, “*Robust Stability Test for Dynamic Systems with Short Delays by Using Padé Approximation*”, Springer, Nonlinear Dynamics, Vol. 18, No. 3, pp. 275-287.

52. **Silva G. J., Datta A., Bhattacharyya S. P., (2005)**, “*PID Controllers for Time-Delay Systems*”, Springer, pp. 77-90.
53. **Meinsma G., Zwart H., (2000)**, “*On H_∞ Control for Dead Time Systems*”, IEEE Transactions on Automatic Control, Vol. 45, No. 2, pp. 272-285.
54. **Meinsma G., Mirkin L., Zhong Q. C., (2002)**, “*A Nehari Theorem for Continuous-Time FIR Systems*”, Notre Dame, USA, Conference Proceedings.
55. **Mirkin L., (2003)**, “*On the Extraction of Dead-Time Controllers and Estimators from Delay-Free Parametrizations*”, IEEE Transactions on Automatic Control, Vol. 48, No. 4, pp. 543-553.

APPENDIX A

CONTROLLER TABLES

<i>Control transfer function</i>	
K_{ff}	$\frac{1431s^3 + 8485s^2 + 1.923 \cdot 10^4 s + 1.433 \cdot 10^4}{s^4 + 1435s^3 + 8489s^2 + 1.923 \cdot 10^4 s + 1.433 \cdot 10^4}$
K_{fb}	$\frac{3150s^3 + 1.337 \cdot 10^4 s^2 + 1.517 \cdot 10^4 s + 3571}{s^4 + 1435s^3 + 8489s^2 + 1.923 \cdot 10^4 s + 1.433 \cdot 10^4}$

Table 1: Controllers computation for experiment of chapter 2.

<i>Control transfer function</i>	
$K_{ff}(0.1)$	$\frac{5.13 \cdot 10^5 s^5 + 1.761 \cdot 10^7 s^4 + 2.182 \cdot 10^8 s^3 + 1.148 \cdot 10^9 s^2 + 2.291 \cdot 10^9 s + 1.496 \cdot 10^9}{s^6 + 1.466 \cdot 10^4 s^5 + 7.373 \cdot 10^6 s^4 + 1.642 \cdot 10^8 s^3 + 1.137 \cdot 10^9 s^2 + 2.329 \cdot 10^9 s + 1.552 \cdot 10^9}$
$K_{fb}(0.1)$	$\frac{7.227 \cdot 10^5 s^5 + 2.373 \cdot 10^7 s^4 + 2.712 \cdot 10^8 s^3 + 1.197 \cdot 10^9 s^2 + 1.379 \cdot 10^9 s + 2.226 \cdot 10^8}{s^6 + 1.466 \cdot 10^4 s^5 + 7.373 \cdot 10^6 s^4 + 1.642 \cdot 10^8 s^3 + 1.137 \cdot 10^9 s^2 + 2.329 \cdot 10^9 s + 1.552 \cdot 10^9}$
$K_{ff}(0.2)$	$\frac{5.317 \cdot 10^5 s^5 + 1.559 \cdot 10^7 s^4 + 1.614 \cdot 10^8 s^3 + 7.058 \cdot 10^8 s^2 + 1.265 \cdot 10^9 s + 7.751 \cdot 10^8}{s^6 + 7610 s^5 + 3.821 \cdot 10^6 s^4 + 8.511 \cdot 10^7 s^3 + 5.892 \cdot 10^8 s^2 + 1.207 \cdot 10^9 s + 8.042 \cdot 10^8}$
$K_{fb}(0.2)$	$\frac{7.49 \cdot 10^5 s^5 + 2.085 \cdot 10^7 s^4 + 1.955 \cdot 10^8 s^3 + 6.907 \cdot 10^8 s^2 + 7.261 \cdot 10^8 s + 1.154 \cdot 10^8}{s^6 + 7610 s^5 + 3.821 \cdot 10^6 s^4 + 8.511 \cdot 10^7 s^3 + 5.892 \cdot 10^8 s^2 + 1.207 \cdot 10^9 s + 8.042 \cdot 10^8}$
$K_{ff}(0.3)$	$\frac{1.845 \cdot 10^5 s^5 + 4.567 \cdot 10^6 s^4 + 3.948 \cdot 10^7 s^3 + 1.437 \cdot 10^8 s^2 + 2.239 \cdot 10^8 s + 1.237 \cdot 10^8}{s^6 + 3545 s^5 + 6.924 \cdot 10^5 s^4 + 1.459 \cdot 10^7 s^3 + 9.847 \cdot 10^7 s^2 + 1.953 \cdot 10^8 s + 1.25 \cdot 10^8}$
$K_{fb}(0.3)$	$\frac{2.243 \cdot 10^5 s^5 + 5.228 \cdot 10^6 s^4 + 4.024 \cdot 10^7 s^3 + 1.142 \cdot 10^8 s^2 + 1.027 \cdot 10^8 s + 1.054 \cdot 10^7}{s^6 + 3545 s^5 + 6.924 \cdot 10^5 s^4 + 1.459 \cdot 10^7 s^3 + 9.847 \cdot 10^7 s^2 + 1.953 \cdot 10^8 s + 1.25 \cdot 10^8}$
$K_{ff}(0.4)$	$\frac{1.88 \cdot 10^5 s^5 + 4.496 \cdot 10^6 s^4 + 3.686 \cdot 10^7 s^3 + 1.241 \cdot 10^8 s^2 + 1.805 \cdot 10^8 s + 9.45 \cdot 10^7}{s^6 + 2714 s^5 + 5.29 \cdot 10^5 s^4 + 1.115 \cdot 10^7 s^3 + 7.523 \cdot 10^7 s^2 + 1.492 \cdot 10^8 s + 9.55 \cdot 10^7}$
$K_{fb}(0.4)$	$\frac{2.284 \cdot 10^5 s^5 + 5.135 \cdot 10^6 s^4 + 3.719 \cdot 10^7 s^3 + 9.487 \cdot 10^7 s^2 + 7.929 \cdot 10^7 s + 8.054 \cdot 10^6}{s^6 + 2714 s^5 + 5.29 \cdot 10^5 s^4 + 1.115 \cdot 10^7 s^3 + 7.523 \cdot 10^7 s^2 + 1.492 \cdot 10^8 s + 9.55 \cdot 10^7}$
$K_{ff}(0.5)$	$\frac{1.915 \cdot 10^5 s^5 + 4.485 \cdot 10^6 s^4 + 3.551 \cdot 10^7 s^3 + 1.128 \cdot 10^8 s^2 + 1.548 \cdot 10^8 s + 7.703 \cdot 10^7}{s^6 + 2217 s^5 + 4.312 \cdot 10^5 s^4 + 9.085 \cdot 10^6 s^3 + 6.132 \cdot 10^7 s^2 + 1.216 \cdot 10^8 s + 7.785 \cdot 10^7}$
$K_{fb}(0.5)$	$\frac{2.328 \cdot 10^5 s^5 + 5.116 \cdot 10^6 s^4 + 3.556 \cdot 10^7 s^3 + 8.353 \cdot 10^7 s^2 + 6.529 \cdot 10^7 s + 6.565 \cdot 10^6}{s^6 + 2217 s^5 + 4.312 \cdot 10^5 s^4 + 9.085 \cdot 10^6 s^3 + 6.132 \cdot 10^7 s^2 + 1.216 \cdot 10^8 s + 7.785 \cdot 10^7}$
$K_{ff}(0.6)$	$\frac{1.952 \cdot 10^5 s^5 + 4.507 \cdot 10^6 s^4 + 3.48 \cdot 10^7 s^3 + 1.057 \cdot 10^8 s^2 + 1.381 \cdot 10^8 s + 6.543 \cdot 10^7}{s^6 + 1886 s^5 + 3.663 \cdot 10^5 s^4 + 7.717 \cdot 10^6 s^3 + 5.209 \cdot 10^7 s^2 + 1.033 \cdot 10^8 s + 6.613 \cdot 10^7}$
$K_{fb}(0.6)$	$\frac{2.372 \cdot 10^5 s^5 + 5.136 \cdot 10^6 s^4 + 3.467 \cdot 10^7 s^3 + 7.622 \cdot 10^7 s^2 + 5.602 \cdot 10^7 s + 5.577 \cdot 10^6}{s^6 + 1886 s^5 + 3.663 \cdot 10^5 s^4 + 7.717 \cdot 10^6 s^3 + 5.209 \cdot 10^7 s^2 + 1.033 \cdot 10^8 s + 6.613 \cdot 10^7}$
$K_{ff}(0.7)$	$\frac{1.991 \cdot 10^5 s^5 + 4.548 \cdot 10^6 s^4 + 3.447 \cdot 10^7 s^3 + 1.01 \cdot 10^8 s^2 + 1.264 \cdot 10^8 s + 5.719 \cdot 10^7}{s^6 + 1652 s^5 + 3.202 \cdot 10^5 s^4 + 6.745 \cdot 10^6 s^3 + 4.553 \cdot 10^7 s^2 + 9.029 \cdot 10^7 s + 5.78 \cdot 10^7}$
$K_{fb}(0.7)$	$\frac{2.419 \cdot 10^5 s^5 + 5.179 \cdot 10^6 s^4 + 3.42 \cdot 10^7 s^3 + 7.122 \cdot 10^7 s^2 + 4.945 \cdot 10^7 s + 4.874 \cdot 10^6}{s^6 + 1652 s^5 + 3.202 \cdot 10^5 s^4 + 6.745 \cdot 10^6 s^3 + 4.553 \cdot 10^7 s^2 + 9.029 \cdot 10^7 s + 5.78 \cdot 10^7}$

Table 2: Controllers computation for first example of chapter 3.

<i>Control design by Smith-predictor</i>	
$K_{ff\circ} = \frac{1431s^3+8485s^2+1.923\ 10^4s+1.433\ 10^4}{s^4+1435s^3+8489s^2+1.923\ 10^4s+1.433\ 10^4}$	
$K_{fb\circ} = \frac{3150s^3+1.337\ 10^4s^2+1.517\ 10^4s+3571}{s^4+1435s^3+8489s^2+1.923\ 10^4s+1.433\ 10^4}$	
<i>Control design by FIR block for 0.1 delay</i>	
$K_{ff\circ} = \frac{1767s^3+1.031\ 10^4s^2+2.271\ 10^4s+1.656\ 10^4}{s^4+1435s^3+8804s^2+2.146\ 10^4s+1.656\ 10^4}$	
$K_{fb\circ} = \frac{3519s^3+1.483\ 10^4s^2+1.654\ 10^4s+3618}{s^4+1435s^3+8804s^2+2.146\ 10^4s+1.656\ 10^4}$	
$\hat{G} = \frac{0.01361s^2-0.25s+2.5}{s^3+2.5s^2}$	
<i>Control design by FIR block for 0.3 delay</i>	
$K_{ff\circ} = \frac{9.118\ 10^7s^3+5.196\ 10^8s^2+1.110^9s+7.76\ 10^8}{s^4+4.706\ 10^7s^3+3.086\ 10^8s^2+9.214\ 10^8s+7.826\ 10^8}$	
$K_{fb\circ} = \frac{1.561\ 10^8s^3+6.508\ 10^8s^2+7.061\ 10^8s+1.361\ 10^8}{s^4+4.706\ 10^7s^3+3.086\ 10^8s^2+9.214\ 10^8s+7.826\ 10^8}$	
$\hat{G} = \frac{0.1468s^2-0.75s+2.5}{s^3+2.5s^2}$	
<i>Control design by FIR block for 0.5 delay</i>	
$K_{ff\circ} = \frac{6931s^3+3.863\ 10^4s^2+7.834\ 10^4s+5.328\ 10^4}{s^4+1523s^3+1.162\ 10^4s^2+5.455\ 10^4s+5.329\ 10^4}$	
$K_{fb\circ} = \frac{9969s^3+4.087\ 10^4s^2+4.227\ 10^4s+6053}{s^4+1523s^3+1.162\ 10^4s^2+5.455\ 10^4s+5.329\ 10^4}$	
$\hat{G} = \frac{0.4961s^2-1.25s+2.5}{s^3+2.5s^2}$	
<i>Control design by a transformed standard H_∞ problem for 0.1 delay</i>	
$K_{ff\circ} = \frac{11.23s^3+46.73s^2+50.55s+9.568}{s^4+12.35s^3+42.91s^2+49.59s+9.568}$	
$K_{fb\circ} = \frac{1.171\ 10^{-7}s^3+4.599\ 10^{-7}s^2+4.181\ 10^{-7}s}{s^4+12.35s^3+42.91s^2+49.59s+9.568}$	
<i>Control design by a transformed standard H_∞ problem for 0.3 delay</i>	
$K_{ff\circ} = \frac{44.04s^3+183s^2+196.7s+36.05}{s^4+34.23s^3+149.2s^2+189.5s+36.05}$	
$K_{fb\circ} = \frac{4.41\ 10^{-7}s^3+1.733\ 10^{-6}s^2+1.575\ 10^{-6}s}{s^4+34.23s^3+149.2s^2+189.5s+36.05}$	
<i>Control design by a transformed standard H_∞ problem for 0.5 delay</i>	
$K_{ff\circ} = \frac{11.23s^3+46.73s^2+50.55s+9.568}{s^4+12.35s^3+42.91s^2+49.59s+9.568}$	
$K_{fb\circ} = \frac{1.171\ 10^{-7}s^3+4.599\ 10^{-7}s^2+4.181\ 10^{-7}s}{s^4+12.35s^3+42.91s^2+49.59s+9.568}$	

Table 3: Controllers computation for experiment of chapter 4.

<i>Second-order Padé-approximation for 0.1 delay</i>	
$K_{ff} =$	$\frac{1768s^7+2.225 \cdot 10^5 s^6+1.187 \cdot 10^7 s^5+3.192 \cdot 10^8 s^4+4.169 \cdot 10^9 s^3+1.822 \cdot 10^{10} s^2+3.511 \cdot 10^{10} s+2.386 \cdot 10^{10}}{s^8+1555s^7+1.871 \cdot 10^5 s^6+9.836 \cdot 10^6 s^5+2.637 \cdot 10^8 s^4+3.468 \cdot 10^9 s^3+1.588 \cdot 10^{10} s^2+3.33 \cdot 10^{10} s+2.386 \cdot 10^{10}}$
$K_{fb} =$	$\frac{3520s^7+4.372 \cdot 10^5 s^6+2.292 \cdot 10^7 s^5+5.979 \cdot 10^8 s^4+7.305 \cdot 10^9 s^3+2.377 \cdot 10^{10} s^2+2.435 \cdot 10^{10} s+5.211 \cdot 10^9}{s^8+1555s^7+1.871 \cdot 10^5 s^6+9.836 \cdot 10^6 s^5+2.637 \cdot 10^8 s^4+3.468 \cdot 10^9 s^3+1.588 \cdot 10^{10} s^2+3.33 \cdot 10^{10} s+2.386 \cdot 10^{10}}$
<i>Second-order Padé-approximation for 0.3 delay</i>	
$K_{ff} =$	$\frac{2956s^5+7.596 \cdot 10^4 s^4+7.663 \cdot 10^5 s^3+2.98 \cdot 10^6 s^2+5.247 \cdot 10^6 s+3.348 \cdot 10^6}{s^6+1456s^5+3.922 \cdot 10^4 s^4+4.257 \cdot 10^5 s^3+1.939 \cdot 10^6 s^2+4.461 \cdot 10^6 s+3.348 \cdot 10^6}$
$K_{fb} =$	$\frac{5040s^5+1.218 \cdot 10^5 s^4+1.115 \cdot 10^6 s^3+3.258 \cdot 10^6 s^2+3.112 \cdot 10^6 s+5.699 \cdot 10^5}{s^6+1456s^5+3.922 \cdot 10^4 s^4+4.257 \cdot 10^5 s^3+1.939 \cdot 10^6 s^2+4.461 \cdot 10^6 s+3.348 \cdot 10^6}$
<i>Second-order Padé-approximation for 0.5 delay</i>	
$K_{ff} =$	$\frac{7480s^5+1.318 \cdot 10^5 s^4+9.503 \cdot 10^5 s^3+3.121 \cdot 10^6 s^2+4.897 \cdot 10^6 s+2.892 \cdot 10^6}{s^6+1452s^5+3.408 \cdot 10^4 s^4+3.236 \cdot 10^5 s^3+1.483 \cdot 10^6 s^2+3.714 \cdot 10^6 s+2.892 \cdot 10^6}$
$K_{fb} =$	$\frac{1.169 \cdot 10^4 s^5+1.887 \cdot 10^5 s^4+1.193 \cdot 10^6 s^3+2.944 \cdot 10^6 s^2+2.563 \cdot 10^6 s+4.138 \cdot 10^5}{s^6+1452s^5+3.408 \cdot 10^4 s^4+3.236 \cdot 10^5 s^3+1.483 \cdot 10^6 s^2+3.714 \cdot 10^6 s+2.892 \cdot 10^6}$
<i>Fifth-order Padé-approximation for 0.1 delay</i>	
$K_{ff} =$	$\frac{1768s^{13}+1.071 \cdot 10^6 s^{12}+3.138 \cdot 10^8 s^{11}+5.824 \cdot 10^{10} s^{10}+7.55 \cdot 10^{12} s^9+7.128 \cdot 10^{14} s^8+4.962 \cdot 10^{16} s^7+2.52 \cdot 10^{18} s^6+9.003 \cdot 10^{19} s^5+2.091 \cdot 10^{21} s^4+2.66 \cdot 10^{22} s^3+1.158 \cdot 10^{23} s^2+2.229 \cdot 10^{23} s+1.515 \cdot 10^{23}}{s^{14}+2035s^{13}+1.044 \cdot 10^6 s^{12}+2.869 \cdot 10^8 s^{11}+5.143 \cdot 10^{10} s^{10}+6.522 \cdot 10^{12} s^9+6.064 \cdot 10^{14} s^8+4.173 \cdot 10^{16} s^7+2.102 \cdot 10^{18} s^6+7.466 \cdot 10^{19} s^5+1.73 \cdot 10^{21} s^4+2.214 \cdot 10^{22} s^3+1.009 \cdot 10^{23} s^2+2.115 \cdot 10^{23} s+1.515 \cdot 10^{23}}$
$K_{fb} =$	$\frac{3520s^{13}+2.127 \cdot 10^6 s^{12}+6.214 \cdot 10^8 s^{11}+1.15 \cdot 10^{11} s^{10}+1.485 \cdot 10^{13} s^9+1.395 \cdot 10^{15} s^8+9.653 \cdot 10^{16} s^7+4.86 \cdot 10^{18} s^6+1.713 \cdot 10^{20} s^5+3.881 \cdot 10^{21} s^4+4.648 \cdot 10^{22} s^3+1.51 \cdot 10^{23} s^2+1.546 \cdot 10^{23} s+3.31 \cdot 10^{22}}{s^{14}+2035s^{13}+1.044 \cdot 10^6 s^{12}+2.869 \cdot 10^8 s^{11}+5.143 \cdot 10^{10} s^{10}+6.522 \cdot 10^{12} s^9+6.064 \cdot 10^{14} s^8+4.173 \cdot 10^{16} s^7+2.102 \cdot 10^{18} s^6+7.466 \cdot 10^{19} s^5+1.73 \cdot 10^{21} s^4+2.214 \cdot 10^{22} s^3+1.009 \cdot 10^{23} s^2+2.115 \cdot 10^{23} s+1.515 \cdot 10^{23}}$
<i>Fifth-order Padé-approximation for 0.3 delay</i>	
$K_{ff} =$	$\frac{2956s^{13}+6.081 \cdot 10^5 s^{12}+6.056 \cdot 10^7 s^{11}+3.828 \cdot 10^9 s^{10}+1.696 \cdot 10^{11} s^9+5.502 \cdot 10^{12} s^8+1.327 \cdot 10^{14} s^7+2.369 \cdot 10^{15} s^6+3.053 \cdot 10^{16} s^5+2.697 \cdot 10^{17} s^4+1.488 \cdot 10^{18} s^3+4.424 \cdot 10^{18} s^2+6.677 \cdot 10^{18} s+3.889 \cdot 10^{18}}{s^{14}+1636s^{13}+3.169 \cdot 10^5 s^{12}+3.104 \cdot 10^7 s^{11}+1.954 \cdot 10^9 s^{10}+8.671 \cdot 10^{10} s^9+2.83 \cdot 10^{12} s^8+6.897 \cdot 10^{13} s^7+1.251 \cdot 10^{15} s^6+1.652 \cdot 10^{16} s^5+1.519 \cdot 10^{17} s^4+8.999 \cdot 10^{17} s^3+3.078 \cdot 10^{18} s^2+5.765 \cdot 10^{18} s+3.889 \cdot 10^{18}}$
$K_{fb} =$	$\frac{5040s^{13}+1.029 \cdot 10^6 s^{12}+1.017 \cdot 10^8 s^{11}+6.369 \cdot 10^9 s^{10}+2.793 \cdot 10^{11} s^9+8.946 \cdot 10^{12} s^8+2.123 \cdot 10^{14} s^7+3.706 \cdot 10^{15} s^6+4.617 \cdot 10^{16} s^5+3.857 \cdot 10^{17} s^4+1.908 \cdot 10^{18} s^3+4.334 \cdot 10^{18} s^2+3.714 \cdot 10^{18} s+6.62 \cdot 10^{17}}{s^{14}+1636s^{13}+3.169 \cdot 10^5 s^{12}+3.104 \cdot 10^7 s^{11}+1.954 \cdot 10^9 s^{10}+8.671 \cdot 10^{10} s^9+2.83 \cdot 10^{12} s^8+6.897 \cdot 10^{13} s^7+1.251 \cdot 10^{15} s^6+1.652 \cdot 10^{16} s^5+1.519 \cdot 10^{17} s^4+8.999 \cdot 10^{17} s^3+3.078 \cdot 10^{18} s^2+5.765 \cdot 10^{18} s+3.889 \cdot 10^{18}}$
<i>Fifth-order Padé-approximation for 0.5 delay</i>	
$K_{ff} =$	$\frac{7481s^{13}+9.397 \cdot 10^5 s^{12}+5.72 \cdot 10^7 s^{11}+2.213 \cdot 10^9 s^{10}+6.021 \cdot 10^{10} s^9+1.204 \cdot 10^{12} s^8+1.804 \cdot 10^{13} s^7+2.02 \cdot 10^{14} s^6+1.661 \cdot 10^{15} s^5+9.662 \cdot 10^{15} s^4+3.728 \cdot 10^{16} s^3+8.673 \cdot 10^{16} s^2+1.096 \cdot 10^{17} s+5.643 \cdot 10^{16}}{s^{14}+1560s^{13}+1.965 \cdot 10^5 s^{12}+1.234 \cdot 10^7 s^{11}+4.974 \cdot 10^8 s^{10}+1.419 \cdot 10^{10} s^9+2.999 \cdot 10^{11} s^8+4.793 \cdot 10^{12} s^7+5.813 \cdot 10^{13} s^6+5.287 \cdot 10^{14} s^5+3.511 \cdot 10^{15} s^4+1.626 \cdot 10^{16} s^3+4.901 \cdot 10^{16} s^2+8.657 \cdot 10^{16} s+5.643 \cdot 10^{16}}$
$K_{fb} =$	$\frac{1.17 \cdot 10^4 s^{11}+1.234 \cdot 10^6 s^{10}+6.09 \cdot 10^7 s^9+1.838 \cdot 10^9 s^8+3.722 \cdot 10^{10} s^7+5.212 \cdot 10^{11} s^6+5.01 \cdot 10^{12} s^5+3.168 \cdot 10^{13} s^4+1.203 \cdot 10^{14} s^3+2.303 \cdot 10^{14} s^2+1.773 \cdot 10^{14} s+2.779 \cdot 10^{13}}{s^{12}+1542s^{11}+1.676 \cdot 10^5 s^{10}+8.779 \cdot 10^6 s^9+2.855 \cdot 10^8 s^8+6.328 \cdot 10^9 s^7+9.926 \cdot 10^{10} s^6+1.109 \cdot 10^{12} s^5+8.665 \cdot 10^{12} s^4+4.54 \cdot 10^{13} s^3+1.498 \cdot 10^{14} s^2+2.856 \cdot 10^{14} s+1.943 \cdot 10^{14}}$

Table 4: Controllers computation for experiment of chapter 4.

APPENDICES B

CURRICULUM VITAE

PERSONAL INFORMATION

Surname, Name: AL-JHAYYISH, Ahmed M. H.
Date and Place of Birth: 28 March 1986, Iraq
Marital Status: Single
Phone: +90 535 686 77 79 / +964 770 911 99 00
Email: ahmed_1986_a@yahoo.com



EDUCATION

Degree	Institution	Year of Graduation
M.Sc.	Çankaya Univ., Electronic & Communication Engineering Dept.	2016
B.Sc.	University of Mosul, College of Electronics Engineering / Electronic Department	2008
High School	Al-Ressala Preparatory School	2004

WORK EXPERIENCE

Year	Place	Enrollment
2009-2012	Al-Buraq Oil Company	Technical Manger

PUBLICATION

Al-Jhayyish A. M. H., Schmidt K. W., (2015), “*Cooperative Adaptive Cruise Control Design for Heterogeneous Vehicle Strings*”, Engineering and Technology symposium in Cankaya University, MTS-8.

LANGUAGES

Native Arabic, Advanced English, Intermediate Turkish

HOBBIES

Travel, Reading, Swimming, Fitness, Football